

Robustness and Infrared Sensitivity of Various Observables in the Application of AdS/CFT to Heavy Ion Collisions

Hong Liu, Krishna Rajagopal and Yeming Shi

*Center for Theoretical Physics,
Massachusetts Institute of Technology,
Cambridge, MA 02139, USA*

E-mail addresses: hong_liu@mit.edu, krishna@ctp.mit.edu, yeming@mit.edu

ABSTRACT: We investigate the robustness with respect to the introduction of nonconformality of five properties of strongly coupled plasmas that have been calculated in $\mathcal{N} = 4$ supersymmetric Yang-Mills (SYM) theory at nonzero temperature, motivated by the goal of understanding phenomena in relativistic heavy ion collisions. (The five properties are the jet quenching parameter, the velocity dependence of screening, and the drag and transverse and longitudinal momentum diffusion coefficients for a heavy quark pulled through the plasma.) We do so using a toy model in which nonconformality is introduced via a one-parameter deformation of the AdS black hole dual to the hot $\mathcal{N} = 4$ SYM plasma. For values of this parameter which correspond to a degree of nonconformality comparable to that seen in lattice calculations of QCD thermodynamics at temperatures a few times that of the crossover to quark-gluon plasma, we find that the jet quenching parameter is affected by the nonconformality at the 30% level or less, the screening length is affected at the 20% level or less, but the drag and diffusion coefficients for a slowly moving heavy quark can be modified by as much as 80%. However, we show that all but one of the five properties that we investigate become completely insensitive to the nonconformality in the high velocity limit $v \rightarrow 1$. The exception is the jet quenching parameter, which is unique among the quantities that we investigate in being “infrared sensitive” even at $v = 1$, where it is defined. That is, it is the only high-velocity observable that we investigate which is sensitive to properties of the medium at infrared energy scales proportional to T , namely the scales where the quark-gluon plasma of QCD can be strongly coupled. The other four quantities all probe only scales that are larger than T by a factor that diverges as $v \rightarrow 1$, namely scales where the $\mathcal{N} = 4$ SYM plasma can be strongly coupled but the quark-gluon plasma of QCD is not.

KEYWORDS: AdS/CFT correspondence, Thermal Field Theory.

Contents

1. Introduction and Summary	1
2. Jet Quenching Parameter	7
2.1 Calculation	8
2.2 Robustness and Infrared Sensitivity	9
3. Heavy quark drag and diffusion from AdS/CFT	12
3.1 Formulation	12
3.2 Finding the Trailing String and Calculating the Drag	13
3.3 Worldsheet Fluctuations	14
3.4 Calculation of κ_T	17
3.5 Calculation of κ_L	19
3.6 Robustness and Infrared Sensitivity	20
4. Quark-Antiquark Potential and Screening Length	22
4.1 Calculating the Potential	23
4.2 Robustness and Infrared Sensitivity of the Screening Length	25
5. Outlook	28
A. Some Technical Details	30
A.1 Technical Details Needed in the Calculation of κ_T	30
A.2 Technical Details Needed in the Calculation of κ_L	32

1. Introduction and Summary

The AdS/CFT correspondence [1] has provided an important tool for understanding the dynamics of many and varied strongly coupled gauge theories. By now, it has been applied at nonzero temperature to gauge theory plasmas in theories that are conformal, or not; theories that are confining at zero temperature, or not; theories with varying degrees of supersymmetry; theories which at weak coupling contain both fundamentals and adjoints, or only adjoints; to plasmas with zero or nonzero chemical potentials; to plasmas that are static or expanding. In terms that are qualitative enough to apply to all these examples, the correspondence states that a (3+1)-dimensional gauge theory plasma at some temperature T is equivalent to a (particular) string theory in a (particular) curved higher-dimensional spacetime which includes a black hole horizon with Hawking temperature T . In the limit in which N_c , the number of colors in the gauge theory, and

$\lambda \equiv g^2 N_c$, the 't Hooft coupling of the gauge theory, are both taken to infinity, the equivalent (dual) gravity description of the strongly coupled gauge theory plasma becomes classical. This means that, in the regime of large N_c and strong coupling, calculations of various dynamical properties of strongly coupled gauge theory plasmas (that are difficult to calculate in the gauge theory *per se*) become equivalent to tractable calculations in a classical spacetime background. We shall specify five examples of such calculations below.

The simplest, most symmetric, example of a gauge theory whose dual gravity description is the original example discussed by Maldacena: $\mathcal{N} = 4$ supersymmetric Yang-Mills theory (SYM), which at nonzero temperature is dual to Type IIB string theory a $(9 + 1)$ -dimensional spacetime given by $(4 + 1)$ -dimensional Anti-de Sitter (AdS) space, with the five remaining compact dimensions forming an S_5 . The metric for the AdS black hole can be written as

$$\begin{aligned}
 ds^2 &= -\frac{r^2}{R^2} \left(1 - \frac{r_0^4}{r^4}\right) dt^2 + \frac{r^2}{R^2} d\vec{x}^2 + \frac{R^2}{r^2} \frac{dr^2}{1 - \frac{r_0^4}{r^4}} \\
 &= \frac{R^2}{z^2} \left[-\left(1 - \frac{z^4}{z_0^4}\right) dt^2 + dx_1^2 + dx_2^2 + dx_3^2 + \frac{dz^2}{1 - \frac{z^4}{z_0^4}} \right], \tag{1.1}
 \end{aligned}$$

where R is the AdS curvature, where $z = R^2/r$, and where the black hole horizon is at $r = r_0 = \pi R^2 T$, meaning $z = z_0 = \frac{1}{\pi T}$. In some respects, the gauge theory can be thought of as living at the $(3 + 1)$ -dimensional “boundary” $z = 0$. However, it is important to remember that the equivalence between the gauge theory and its gravity description is holographic, in that all of the physics at varying values of z in the gravity description is encoded in the gauge theory, with the fifth-dimension-position z in the spacetime (1.1) corresponding to length scale in the $(3 + 1)$ -dimensional gauge theory [1, 2].

Although many (in fact infinitely many) other examples of gauge theories with dual gravity descriptions are known, such a description has not yet been found for $SU(N_c)$ gauge theory (with or without quarks in the fundamental representation). And, furthermore, all known theories with gravity duals differ from QCD in important respects. Taking $\mathcal{N} = 4$ SYM as an example, at weak coupling it has more adjoint degrees of freedom than in QCD, it has no fundamental degrees of freedom, and it is conformal. And, at zero temperature $\mathcal{N} = 4$ SYM is supersymmetric and does not feature either confinement or chiral symmetry breaking. However, the plasmas of the two theories, namely $\mathcal{N} = 4$ SYM at $T > 0$ and QCD at T above $T_c \sim 170$ MeV, are more similar than their vacua. Neither plasma confines or breaks chiral symmetry, and neither is supersymmetric since $T \neq 0$ breaks supersymmetry. The successful comparison of data from heavy ion collisions at RHIC (on azimuthally asymmetric collective flow) with ideal (zero shear viscosity η) hydrodynamics indicates that, somewhat above T_c , the QCD plasma is a strongly coupled liquid [3]. Strongly coupled liquids may not have any well-defined quasiparticles, so the differences between the quasiparticles of the two theories at weak coupling need not be important, at least for judiciously chosen ratios of observables. And, lattice calculations [4, 5, 6, 7] indicate that above $\sim 2T_c$, the thermodynamics of the QCD plasma becomes approximately scale invariant. More generally speaking, it is often the case that macroscopic phenomena in a sufficiently excited many-body system are common across large universality classes of theories that differ in many (microscopic) respects. This raises the

exciting possibility that one may be able to gain insights into the thermodynamics and dynamics of the strongly coupled plasma of QCD using calculations in other gauge theories whose gravity duals are currently known.

Many authors have developed the strategy of calculating dynamical properties of gauge theory plasmas (that are of interest because they can be related to phenomena in heavy ion collision experiments) by calculating them in $\mathcal{N} = 4$ SYM and other theories with gravity duals. Turning the qualitative insights obtained in this way into semiquantitative inferences for QCD (or even for QCD at large N_c) requires understanding what observables are universal across what classes of strongly coupled plasmas or, if not that, understanding how observables change as the strongly coupled $\mathcal{N} = 4$ SYM plasma is deformed in various ways that make it more QCD-like. At present, the quantity for which the evidence of a universality of this sort is strongest is η/s , the ratio of the shear viscosity to the entropy density: in the large N_c and strong coupling limit, it is given by $1/4\pi$ for *any* gauge theory with a dual gravity description [8, 9, 10]. The discovery that in an infinite class of conformal gauge theories the jet quenching parameter \hat{q} , that we shall discuss below, is given by $\sqrt{\lambda}T^3$ times a pure number that is proportional to \sqrt{s}/N_c suggests a second quantity with a degree of universality [11], but one that at present is only known to apply to conformal theories.

It is clearly critical to extend AdS/CFT calculations of dynamical properties of gauge theory plasmas to nonconformal theories. Unfortunately, the known examples of nonconformal gauge theories with gravity duals are rather complicated at nonzero temperature, see for example Refs. [12, 13], making it hard to extract insights from them without extensive, probably numerical, study. Here we will take a pragmatic approach, using a simple toy model, similar to that introduced at zero temperature in Ref. [14] and at nonzero temperature in Refs. [15, 16] and in the form that we shall use by Kajantie, Tahkokallio and Yee [17], in which (1.1) is deformed into the string frame metric

$$\begin{aligned} ds^2 &= \frac{R^2 e^{\frac{29cz^2}{20}}}{z^2} \left[- \left(1 - \frac{z^4}{z_0^4} \right) dt^2 + dx_1^2 + dx_2^2 + dx_3^2 + \frac{dz^2}{1 - \frac{z^4}{z_0^4}} \right] \\ &= e^{\frac{29}{20}c\frac{R^4}{r^2}} \left[- \frac{r^2}{R^2} \left(1 - \frac{r_0^4}{r^4} \right) dt^2 + \frac{r^2}{R^2} d\vec{x}^2 + \frac{R^2}{r^2} \frac{dr^2}{1 - \frac{r_0^4}{r^4}} \right]. \end{aligned} \quad (1.2)$$

Here, the dimensionful quantity c defines a one-parameter nonconformal deformation of the AdS black hole. Certainly our investigations should also be repeated for other examples of such deformations. The advantage of using the specific form (1.2) is its tractability together with the fact that the authors of Ref. [17] have estimated that choosing $c \simeq 0.127 \text{ GeV}^2$ makes the thermodynamics of this toy model most similar to QCD thermodynamics, determined by lattice calculations. Specifically, they introduce a second toy model for QCD below T_c , choose its parameters to give a reasonable meson spectrum in vacuum, and then find that $c = 0.127 \text{ GeV}^2$ puts the transition between their low and high temperature models — whose construction is their purpose — at $T_c = 170 \text{ MeV}$, as in QCD.

We shall determine how five dynamical observables, previously calculated at $c = 0$, depend on c . Since in the absence of c the only dimensionful quantity in the otherwise conformal theory is T , the magnitude of the nonconformal effects that we compute must be controlled by the dimensionless

ratio c/T^2 . We shall plot our results for values of this parameter that lie within the range $0 \leq c/T^2 \leq 4$, which corresponds to allowing a c as large as 0.36 GeV^2 at $T = 300 \text{ MeV}$. Note that the metric (1.2) does not correspond to a solution to supergravity equations of motion, and note furthermore that the form of the metric for the five compact dimensions is unspecified. These ambiguities are what make the model a model: with $c \neq 0$, it is impossible to say what, if any, gauge theory the metric (1.2) is dual to. This makes it impossible to give a rigorous determination of its entropy density s , as the authors of Ref. [17] explain, or to determine its weak coupling degrees of freedom. So, we shall not use this model to test how other observables depend on these quantities. Our sole purpose is to explore the effects of the introduction of nonconformality.

Although it is not possible to give a rigorous argument for the entropy density s corresponding to the metric (1.2), given that the metric is not known to be a solution to supergravity equations of motion, the authors of Ref. [17] have conjectured that s is given by

$$s = \frac{\pi^2 N_c^2 T^3}{2} \exp\left(-\frac{3}{2\pi^2} \frac{c}{T^2}\right). \quad (1.3)$$

We can use this expression to estimate the range of values of c that compare reasonably to QCD thermodynamics, as follows. We take this expression and obtain the energy density ε from $d\varepsilon/dT = Tds/dT$, the pressure $P = Ts - \varepsilon$, and then $(\varepsilon - 3P)/\varepsilon$ which is a measure of nonconformality. We then find that fitting the results for this quantity in the toy model we are using to the lattice calculations of this quantity in QCD from Ref. [5] requires c varying from $c \approx 0.18 \text{ GeV}^2$ at $T = 300 \text{ MeV}$ to $c \approx 0.11 \text{ GeV}^2$ at $T = 700 \text{ MeV}$, and $c \simeq 0.13 \text{ GeV}^2$ does reasonably well over this entire temperature range. This gives us further confidence that when we plot our results over the range $0 \leq c/T^2 \leq 4$ we are turning on a degree of nonconformality that encompasses and exceeds that observed in QCD thermodynamics at $T = 300 \text{ MeV}$. At this temperature, the range $0.11 \text{ GeV}^2 < c < 0.18 \text{ GeV}^2$ corresponds to $1.2 < c/T^2 < 2.0$. Keep in mind that although c is the fixed parameter in the model, it will enter all of our results through the dimensionless parameter c/T^2 . So, when we plot our results over $0 < c/T^2 < 4$, we can think of the higher (lower) values of c/T^2 as corresponding to lower (higher) temperatures.

We shall calculate five quantities that have previously been argued to be of interest because, in QCD, they are related to phenomena in heavy ion collision experiments. We begin in Section 2 by calculating the jet quenching parameter \hat{q} , as in Refs. [18, 19, 11]. This property of the strongly coupled plasma enters into the description of how a parton moving through this plasma with energy E loses energy by radiating gluons [20, 21, 22]. Gluon radiation is the dominant energy loss mechanism in the limit where $E \gg k_T \gg T$, with k_T being the typical transverse momentum of the radiated gluons, and upon assuming that $\alpha_s(k_T)$ is small [20, 21, 22, 23, 24]. That is, the analysis of jet quenching in this limit is based upon the assumption that QCD can be considered weakly coupled at the scale k_T , even though its quark-gluon plasma (at scales $\sim T$) is strongly coupled. In this regime, the gluon radiation itself is described via a weakly coupled QCD formalism in which the one property of the thermal medium that enters is \hat{q} , which must be computed at strong coupling. In Section 3, we turn to probes of the plasma in a completely different kinematic regime. We shall calculate three observables that describe the motion of a heavy enough quark (mass M) moving through the strongly coupled plasma with a low enough velocity v , where the

criterion that must be satisfied by M and v is [25, 26, 11]

$$M > \frac{\sqrt{\lambda}T}{(1 - v^2)^{1/4}}. \quad (1.4)$$

Because we are no longer taking the $v \rightarrow 1$ limit, even in a theory like QCD that is weakly coupled in the ultraviolet we cannot assume that energy loss is dominated by gluon radiation and cannot assume that there is a separation of scales which justifies treating a part of the problem at weak coupling even when the plasma itself is strongly coupled. Instead, it is worth investigating a formalism in which the entire calculation is done at strong coupling. In the dual gravity theory, the criterion (1.4) corresponds to requiring that the velocity of the quark not exceed the local speed of light at the position in z where quarks of mass M are located. When (1.4) is satisfied, the moving quark is described in the dual gravity theory as trailing a string that drags behind the moving quark [27, 28], meaning that the quark feels a drag force and diffuses. The three parameters that we calculate are the drag coefficient μ (introduced and calculated at $c = 0$ in [27, 28]) and the diffusion constants κ_T and κ_L for its transverse and longitudinal motion (introduced and calculated at $c = 0$ in [29, 25, 26]). The effects of the nonconformal deformation of the AdS black hole metric on both μ and \hat{q} have been calculated previously in Ref. [16]. Finally, in Section 4 we determine how c affects the velocity dependence of the screening length L_s defined by the potential between a quark-antiquark pair with mass M moving through the plasma with velocity v [30, 31, 32, 11], again satisfying (1.4) which in this case corresponds to the requirement that L_s be greater than the Compton wavelength of an individual quark [11]. We shall show that, for $0 < c/T^2 < 4$, the effects of c on the jet quenching parameter and on the screening length are modest. For example, \hat{q} increases by about 14% (28%) for $c/T^2 = 2$ ($c/T^2 = 4$) while the screening length increases by about 9% (20%). This indicates that these quantities are robust against introduction of nonconformality to a degree larger than that indicated by lattice study of QCD thermodynamics. The drag coefficient and the two momentum diffusion constants for a heavy slowly moving quark are somewhat less robust, increasing by about 34% (80%) for $c/T^2 = 2$ ($c/T^2 = 4$). Of course, our conclusions are only quantitative within one toy model. Other examples in which nonconformality is introduced should also be studied.

The metric (1.2) has the feature that it becomes the metric (1.1) of an AdS black hole near $z = 0$, but near the horizon it is modified by the dimensionful parameter c . This allows us to address a further issue, that is both qualitative and important. QCD, being asymptotically free, is weakly coupled in the ultraviolet. The plasma in a strongly coupled conformal theory like $\mathcal{N} = 4$ SYM is strongly coupled in the ultraviolet as well as at scales of order T . This means that the only properties of the plasma in a strongly coupled conformal gauge theory that may yield insight into the strongly coupled plasma of QCD are those properties which are determined by the physics at scales of order T , not by the ultraviolet physics. It is impossible to use calculations done within $\mathcal{N} = 4$ SYM to determine which quantities are “infrared sensitive” in this sense, precisely because the theory is conformal: the parameter z_0 specifies the location of the horizon and the value of the temperature $T = 1/(\pi z_0)$, namely the gauge theory physics at scales $\sim T$, and at the same time specifies the form of the metric (1.1) at small z , namely the gauge theory physics in the ultraviolet. So, seeing z_0 and hence T occurring in the calculated results for \hat{q} , μ , κ_T , κ_L and L_s in $\mathcal{N} = 4$ SYM

does not allow us to determine whether any of these quantities are infrared sensitive. In order to make such a determination, we must modify the theory in the infrared, i.e. in the vicinity of $z = z_0$, in a way that leaves it unmodified at $z \rightarrow 0$, and determine which quantities are modified and which not. Note that in a gauge theory whose gravity dual is given asymptotically (i.e. at $z \rightarrow 0$) by the AdS black hole metric (1.1), the parameter z_0 that occurs in the asymptotic metric will, in the generic case, not be related to the temperature in any simple way. Absent conformality, there is no longer any reason for the true temperature T , defined by the metric at the horizon, to be related in any simple way to the parameter z_0 defined by the AdS black hole metric at $z \rightarrow 0$.¹ Our toy model is not generic enough to manifest this effect — the temperature remains $1/(\pi z_0)$ even when $c \neq 0$ — but we can nevertheless use the dependence on c/T^2 to diagnose infrared sensitivity.

We find that \hat{q} is infrared sensitive — as noted above it changes by 28% for $c/T^2 = 4$. The other four quantities that we study are all infrared sensitive at low velocity. However, if we take $v \rightarrow 1$ and $M \rightarrow \infty$ while maintaining the criterion (1.4) — for example by taking $M \rightarrow \infty$ first — we find that μ , κ_T , κ_L and L_s all become infrared *insensitive*. That is, they become independent of c/T^2 in this limit, meaning that they cannot see a modification of the gauge theory at scales $\sim T$. In this $v \rightarrow 1$ limit, they are determined entirely by the ultraviolet physics in the gauge theory, making it unlikely that their calculation in $\mathcal{N} = 4$ SYM in this limit can be used to draw quantitative lessons for QCD. The jet quenching parameter, on the other hand, is defined at $v \equiv 1$ and is infrared sensitive. This is consistent with its role in jet quenching calculations as the parameter through which the physics of the strongly coupled plasma at scales of order the temperature enters into the calculation of how partons moving through this plasma lose energy in the high parton energy limit.

At a qualitative level, our results for the infrared sensitivity of all five observables can be guessed by examining how they are computed in the strongly coupled $\mathcal{N} = 4$ SYM theory. The jet-quenching parameter \hat{q} is extracted from the short-transverse-distance behavior of the thermal expectation value of a light-like Wilson loop that is long in light-like extent but short in transverse extent. In the dual gravity description, this expectation value can be calculated by finding the extremal configuration of a string connecting a quark-anti-quark pair moving at the speed of light. The extremal string configuration touches the horizon [18]. In the short transverse distance limit, after subtracting the self-energy of each quark, one is left with mostly the contribution of the part of the extremal string worldsheet that is near the horizon. It is therefore reasonable that, upon calculation, we find that \hat{q} is infrared sensitive, as is also expected given the role that it plays in the theory of jet quenching. In contrast, a heavy quark moving through the hot plasma with velocity v , satisfying (1.4), is described by the trailing string worldsheet first analyzed in Refs. [27, 28] which has a “worldsheet horizon” on it located at $z = z_0(1 - v^2)^{1/4}$ as described in Refs. [25, 26]. The quantities μ , κ_T and κ_L are determined by the string worldsheet outside the worldsheet horizon, namely in the region $0 < z < z_0(1 - v^2)^{1/4}$. (μ is determined by the momentum flow along the string worldsheet outside the worldsheet horizon; the diffusion constants κ_T and κ_L are determined from two-point functions describing the fluctuations of the worldsheet coordinates outside the worldsheet horizon.) So, if we take the $v \rightarrow 1$ limit (while increasing M so as to

¹Consider the $(4 + 1)$ -dimensional extremal Reissner-Nordstrom black hole as an example that is not directly relevant but in which this disconnect is particularly dramatic: the asymptotic metric for this spacetime defines a z_0 , but the Hawking temperature is zero.

maintain (1.4)) we expect these quantities to become completely infrared *insensitive*, sensitive only to the ultraviolet physics. Our explicit calculation confirms this expectation. The argument for the screening length is similar. As $v \rightarrow 1$ (while maintaining (1.4)) the velocity dependent screening length shrinks, $L_s(v) \sim L_s(0)(1 - v^2)^{1/4}$ [30, 31, 32, 11], and the string worldsheet bounded by the quark-antiquark pair — which determines the potential and hence L_s — only explores the $(4 + 1)$ -dimensional spacetime in the region $0 < z \lesssim z_0(1 - v^2)^{1/4}$. We therefore also expect, and find, that L_s is infrared insensitive in the $v \rightarrow 1$ limit. It is worth noting, however, that for charmonium (or bottomonium) mesons with velocities corresponding to the transverse momenta with which they are produced in RHIC (or LHC) collisions, L_s remains infrared sensitive, probing the strongly coupled medium at scales not far above T . And, the velocity-dependence of the screening length is described reasonably well by $L_s(v) \sim L_s(0)(1 - v^2)^{1/4}$ at all velocities, large or small, up to corrections that we shall evaluate.

So, the five quantities that we investigate are robust to varying degrees, in the sense that if we turn on nonconformality parametrized by a value of c/T^2 that is about twice as large as that which best approximates QCD thermodynamics at $T = 300$ MeV within the model of Ref. [17], the jet quenching parameter increases by about 30% and at low velocities the screening length increases by about 20% while the heavy quark drag and momentum diffusion coefficients increase by about 80%. If we then take the limit $v \rightarrow 1$ while increasing the quark mass M so as to maintain (1.4), we find that the drag and diffusion coefficients and the screening length all become completely insensitive to the nonconformal modification of the physics at scales $\sim T$ that we have introduced. In this limit, these quantities all become infrared insensitive. This makes it likely that the calculation of these quantities in a conformal theory like $\mathcal{N} = 4$ SYM can only be used to learn about the strongly coupled plasma of QCD at a broadly qualitative level. In contrast, the jet quenching parameter \hat{q} is defined at $v \equiv 1$ and is infrared sensitive, probing the properties of the plasma at scales of order the temperature where it is strongly coupled in both QCD and $\mathcal{N} = 4$ SYM.

2. Jet Quenching Parameter

The jet quenching parameter \hat{q} is the property of the plasma that enters into the description of how a parton moving through this plasma with energy E loses energy by radiating gluons with typical transverse momentum k_T in the limit where $E \gg k_T \gg T$ and upon assuming that $\alpha_s(k_T)$ is small enough that QCD can be considered weakly coupled at this scale, even though its quark-gluon plasma (at scales $\sim T$) is strongly coupled [20, 21, 22, 23, 24]. To the degree that these assumptions are valid, parton energy loss is dominated by gluon radiation. In experiments at RHIC, the jets studied correspond to partons with E at most a few tens of GeV [3]. At the LHC, although the quark-gluon plasma being studied is likely to be at most a factor of two hotter than that at RHIC, the jets whose quenching will be studied will have energies of a few hundreds of GeV [33], putting the assumptions upon which the definition and extraction of the jet quenching parameter is based on more quantitative footing.

If the quark-gluon plasma were weakly coupled, \hat{q} would be proportional to $\mu^2/\tilde{\lambda}$, where μ is the inverse of the Debye screening length and $\tilde{\lambda}$ is a suitably defined mean free path for weakly coupled quasiparticles [20]. Up to a logarithm, in a weakly coupled quark-gluon plasma $\hat{q} \propto g^4 N_c^2 T^3$ [20, 34].

Wiedemann observed that, still for a weakly coupled plasma, \hat{q} can instead be extracted from the small- L behavior of a rectangular adjoint Wilson loop whose long sides, of length L^- , are light-like and whose short sides, of length L , are transverse to the light-cone [22]. L^- corresponds to the extent of the medium through which the radiated gluon travels and $1/L$ corresponds to the transverse momentum of the radiated gluon. Wiedemann and two of us suggested that this definition can be generalized to a strongly coupled plasma, and calculated \hat{q} for the strongly coupled $\mathcal{N} = 4$ SYM plasma [18]. In this section, we repeat this calculation of \hat{q} for the metric (1.2) of Ref. [17], deformed to introduce nonconformality.

2.1 Calculation

In the large N_c limit, the expectation value of the adjoint Wilson loop is the square of that in the fundamental representation. If we in addition take the large λ limit and use the AdS/CFT correspondence, the expectation value of the Wilson loop in the fundamental representation can be computed as [35, 36]

$$\langle W(C) \rangle = e^{iS_I}, \quad S_I = S(C) - 2S_0, \quad (2.1)$$

where $S(C)$ is the Nambu-Goto action for the extremal worldsheet bounded at $z = 0$ by the Wilson loop contour C and S_0 is the Nambu-Goto action for an individual quark. For a rectangular Wilson loop extending a distance L^- along the x^- light-like direction and a distance L along a transverse direction, in the regime $L^- \gg 1/T \gg L$ the expectation value of the Wilson loop in the fundamental representation takes the form [18, 11]

$$\langle W(C) \rangle \equiv e^{-\frac{1}{8\sqrt{2}}\hat{q}L^-L^2}, \quad (2.2)$$

which defines the relation between the jet quenching parameter \hat{q} and the Wilson loop. Let us consider a more general non-conformal metric of the form

$$ds^2 = g(r) \left[-(1 - f(r))dt^2 + d\vec{x}^2 \right] + \frac{1}{h(r)}dr^2, \quad (2.3)$$

which includes both (1.1) and (1.2) as special cases. Buchel demonstrated in [19] that in the generic spacetime metric given by (2.3), the extremal string worldsheet connecting a light-like quark-antiquark pair always touches the horizon, as had been demonstrated in Ref. [18] for the AdS black hole (1.1). And, furthermore, Buchel showed that upon evaluating the Wilson loop the jet quenching parameter \hat{q} is given in terms of the string tension $1/(2\pi\alpha')$ and the functions appearing in the generic metric (2.3) by

$$\hat{q} = \frac{1}{\pi\alpha'} \left(\int_{r_0}^{\infty} \frac{dr}{\sqrt{fg^3h}} \right)^{-1}, \quad (2.4)$$

where r_0 is the coordinate of the black hole horizon. The metric (1.2) corresponds to

$$\begin{aligned} g(r) &= \frac{r^2}{R^2} e^{\frac{29}{20} c \frac{R^4}{r^2}} , \\ f(r) &= \frac{r_0^4}{r^4} , \\ h(r) &= \frac{r^2}{R^2} \left(1 - \frac{r_0^4}{r^4} \right) e^{-\frac{29}{20} c \frac{R^4}{r^2}} , \end{aligned} \tag{2.5}$$

and we shall assume that R is related to λ by $R^2/\alpha' = \sqrt{\lambda}$.² Hence, we find that in the metric (1.2) the jet quenching parameter is given by

$$\begin{aligned} \hat{q} &= \frac{R^4}{\pi\alpha'} \left(\int_{r_0}^{\infty} dr \frac{e^{-\frac{29}{20} c \frac{R^4}{r^2}}}{r_0^2 \sqrt{r^4 - r_0^4}} \right)^{-1} \\ &= \sqrt{\lambda} \pi^2 T^3 \left(\int_1^{\infty} dx \frac{e^{-\frac{29c}{20\pi^2 T^2 x^2}}}{\sqrt{x^4 - 1}} \right)^{-1} , \end{aligned} \tag{2.6}$$

where we have used $r_0 = \pi R^2 T$. The integral in (2.6) can be evaluated analytically, and the result involves modified Bessel functions of the first kind [16]. With $c = 0$, it is given by $\sqrt{\pi} \Gamma(\frac{5}{4}) / \Gamma(\frac{3}{4})$ which yields \hat{q} for $\mathcal{N} = 4$ SYM theory [18]. The result (2.6) was obtained previously in Ref. [16].

From (2.6) we see that $\hat{q} \propto \lambda^{\frac{1}{2}} N_c^0$ meaning that, with $c \neq 0$ as with $c = 0$, the jet quenching parameter is not proportional to the entropy density or to the number density of scatterers or quasiparticles as at weak coupling [18], consistent with the absence of any quasiparticle description of the strongly coupled plasma. Within the formalism of Ref. [37], this qualitative conclusion can be phrased as the statement that multiple gluon correlations are just as important as two gluon correlations in the plasma of strongly coupled $\mathcal{N} = 4$ SYM. And, it is further highlighted by the result that the ratios of the jet quenching parameters of different strongly coupled conformal theories are given by the ratios of the square roots of their entropy densities [11].

In Fig. 1, we plot the dimensionless quantity $\hat{q}/(\sqrt{\lambda} T^3)$ against the dimensionless quantity c/T^2 , through which nonconformality enters the calculation. The dependence on c/T^2 is almost linear over the range of c/T^2 that is of interest, and \hat{q} increases only by about 28% even for the large value $c/T^2 = 4$.

2.2 Robustness and Infrared Sensitivity

Recall from Section 1 that the authors of the model (1.2) find that $c = 0.127 \text{ GeV}^2$ best reproduces certain aspects of QCD thermodynamics known from lattice calculations [17]. And, recall that we

²Since the metric (1.2) reduces to the AdS black hole metric (1.1) at small z — in the ultraviolet in the field theory — the relation between R and λ is $R^2/\alpha' = \sqrt{\lambda}$ in the ultraviolet. If we knew to what field theory the deformed metric (1.2) is dual, i.e. if we knew what the action was whose supergravity equations of motion were solved by (1.2), we can presume that λ would run in some way. As (1.2) is just a toy model that we are using to introduce nonconformality, we cannot determine how λ runs. So, we shall use $R^2/\alpha' = \sqrt{\lambda}$ throughout.

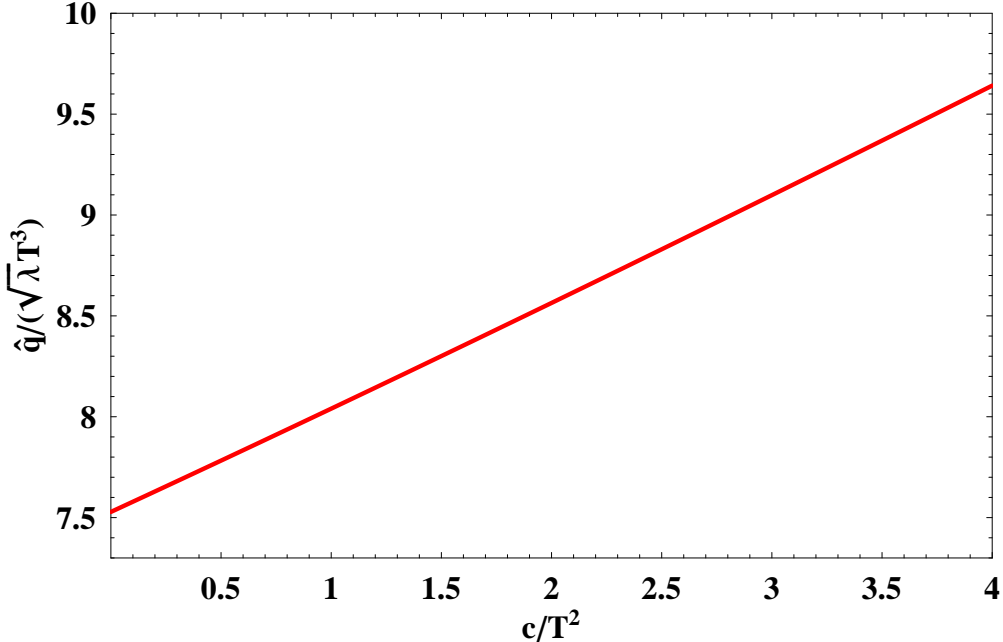


Figure 1: The dependence of the jet quenching parameter on the nonconformality in the metric (1.2). We plot $\hat{q}/(\sqrt{\lambda}T^3)$ versus c/T^2 .

found that the range $0.11 \text{ GeV}^2 < c < 0.18 \text{ GeV}^2$ yielded a degree of nonconformality, parameterized by $(\varepsilon - 3P)/\varepsilon$, as in lattice QCD calculations. By plotting \hat{q} for values of c/T^2 up to 4, at $T = 300 \text{ MeV}$ we are allowing for values of c at least twice as large as is favored by QCD thermodynamics. We see from Fig. 1 that even over this wide range of c/T^2 , the jet quenching parameter is at most increased by less than 30%. If we take $c = 0.13 \text{ GeV}^2$, the increase in \hat{q} is $\sim 10\%$ at $T = 300 \text{ MeV}$ and $\sim 23\%$ at $T = 200 \text{ MeV}$. We see first of all that the $\mathcal{N} = 4$ SYM result is robust: upon varying the degree of nonconformality c/T^2 across a wide range, we find only a small increase in \hat{q} . Second of all, the fact that \hat{q} increases as we turn on c/T^2 is interesting. Among conformal theories, if we reduce the number of degrees of freedom (with fermions weighted by a $7/8$ as in the entropy density) by a factor of $47.5/120$, i.e. as if going from $\mathcal{N} = 4$ SYM with $N_c = 3$ to QCD, \hat{q} is reduced by a factor of $\sqrt{47.5/120} \sim 0.63$ [11]. We now see that this decrease may be partially compensated by an increase in \hat{q} attributable to the nonconformality of QCD. Our result that \hat{q} increases with increasing nonconformality has of course only been obtained in a particular toy model; further investigation in other examples of nonconformal plasmas is called for. One result that corroborates the sign of the effect of nonconformality on \hat{q} is the determination that introducing nonzero R -charge chemical potential(s) in $\mathcal{N} = 4$ SYM, which introduces nonconformality, increases \hat{q} [38]. (See also Ref. [39].) There is one nonconformal strongly coupled plasma in a (3+1)-dimensional gauge theory other than $\mathcal{N} = 4$ SYM for which \hat{q} is known: in the cascading gauge theory of Refs. [40, 12], $\hat{q}/(\sqrt{\lambda}T^3)$ decreases with decreasing temperature, which corresponds to simultaneously decreasing number of degrees of freedom and increasing nonconformality [19]. Further exploring (and separating) the effects of varying numbers of degrees of freedom and varying degrees of nonconformality on \hat{q}

requires calculating this quantity for other nonconformal strongly coupled plasmas, for example that in $\mathcal{N} = 2^*$ SYM [13]. Certainly at present the indications are that all these effects only modify \hat{q} at the few tens of percent level, a robustness that is supported by the present investigation of the effects of nonconformality alone in a toy model. If further study continues to support the idea that in going from $\mathcal{N} = 4$ SYM to QCD the jet quenching parameter decreases by a factor $\sqrt{47.5/120} \sim 0.63$ by virtue of the decrease in degrees of freedom and increases by a few tens of percent by virtue of the nonconformality of the QCD plasma at the temperatures of about $(1.5 - 2)T_c$ explored at RHIC, then the observation [18] that \hat{q} of $\mathcal{N} = 4$ SYM theory at $T = 300$ MeV is in the same ballpark as the range for the time-averaged \bar{q} extracted in comparison with RHIC data [41] will grow in importance.³

Our results confirm that \hat{q} is an infrared sensitive quantity. That is, when we introduce $c/T^2 \neq 0$, modifying the AdS black hole metric at scales of order T but leaving it unmodified in the ultraviolet, we find that \hat{q} is affected by this modification. This is consistent with the interpretation of \hat{q} as the parameter through which the physics of the strongly coupled medium at scales of order the temperature enters into the calculation of radiative parton energy loss and jet quenching. The infrared sensitivity of \hat{q} comes about in its computation because in the gravity dual \hat{q} is described by a string that extends all the way from the ultraviolet regime to the black hole horizon, probing the gauge theory at all scales down to of order the temperature.⁴

³Note also that in going from RHIC to the LHC the dominant change in \hat{q} will come from its T^3 dependence. If we neglect any smaller changes due to decreases in $\sqrt{\lambda}$ and the degree of nonconformality, we predict that in going from RHIC to the LHC the increase in \hat{q} should be proportional to the increase in multiplicity at mid-rapidity [42]. That is, we predict that the time-averaged \bar{q} extracted in comparison with LHC data should be greater than that extracted in comparison with RHIC data by the factor $(dN^{\text{LHC}}/d\eta)/(dN^{\text{RHIC}}/d\eta)$ [42].

⁴In addition to the string worldsheet that determines \hat{q} , the light-like Wilson loop also bounds an extremal world sheet that explores the field theory only on scales comparable to, and to the ultraviolet of, the Compton wavelength of the test quark whose mass is taken to infinity in defining the Wilson loop [18, 43, 11, 44, 45]. When written in terms of the parameter z_0 , the action of this string is identical for any metric that becomes the AdS metric (1.1) asymptotically in the ultraviolet [45], meaning that it is infrared insensitive [11]. As we discussed in Section 1, in any theory that is described by a generic metric that becomes the AdS metric (1.1) with parameter z_0 in the ultraviolet, any quantity that is specified in terms of z_0 rather than by the temperature (which is determined by the metric near the horizon and is in general not related to the ultraviolet parameter z_0 in any simple way) is infrared insensitive. Thus, the explicit calculations of Ref. [45] demonstrate quantitatively that this string solution only probes physics at and beyond the ultraviolet cutoff and is completely insensitive to physics of the strongly coupled plasma at scales of order the temperature. The two different string world sheets bounded by the light-like Wilson loop can be thought of as different saddle points in its Minkowski-space path integral representation. This is a Minkowski-space path integral, with an integrand (proportional to e^{iS}) that is complex for real field configurations (which have real S). It is defined by analytic continuation, with each of the integrals that make up the path integral now a contour integral over the complexified configuration space. In this context, there is no way to use the (imaginary) values of the actions of the two saddle points to determine which dominates the path integral. In the absence of information about which saddle points lie on the infinite dimensional analogue of the path of steepest descent, one must use physical considerations. The calculations of Ref. [45] provide strong evidence confirming previous physical arguments: the infrared insensitive string world sheet does not contribute to the evaluation of the Wilson loop, and hence \hat{q} [18, 11].

3. Heavy quark drag and diffusion from AdS/CFT

3.1 Formulation

The relativistic generalization of the Langevin equations for a heavy quark moving through some thermal medium (see for example Refs. [46, 29]) can be written as

$$\frac{dp_L}{dt} = -\mu(p_L)p_L + \xi_L(t) , \quad (3.1)$$

$$\frac{dp_T}{dt} = \xi_T(t) , \quad (3.2)$$

where p_L and p_T are the longitudinal and transverse momentum of the quark, respectively. (We have simplified the notation by dropping the spatial indices on transverse quantities.) Henceforth, we shall denote p_L by p . ξ_L and ξ_T are random fluctuating forces in the longitudinal and transverse directions, which satisfy

$$\langle \xi_L(t)\xi_L(t') \rangle = \kappa_L(p)\delta(t-t') , \quad (3.3)$$

$$\langle \xi_T(t)\xi_T(t') \rangle = \kappa_T(p)\delta(t-t') . \quad (3.4)$$

$\kappa_L(p)$ and two times $\kappa_T(p)$ describe how much longitudinal and transverse momentum squared is transferred to the quark per unit time. Note that at zero velocity, $\kappa_L(0) = \kappa_T(0)$ whereas for $p > 0$ one expects that $\kappa_L(p) \neq \kappa_T(p)$. Also, upon assuming that the momentum fluctuations of the particle are in equilibrium with the thermal medium, as appropriate at zero velocity, a fluctuation-dissipation theorem relates $\mu(0)$ to $\kappa_L(0)$ via the Einstein relation

$$\mu(0) = \frac{\kappa_L(0)}{2MT} , \quad (3.5)$$

where M is the static mass of the quark. The relation (3.5) is not expected to hold for $p > 0$.

To compute the various quantities $\mu(p)$, $\kappa_T(p)$ and $\kappa_L(p)$ in the metric (1.2), we use the following procedure developed in Refs. [29, 25, 26]:

1. Find a classical solution to the Nambu-Goto action

$$S_{NG} = \frac{1}{2\pi\alpha'} \int d\tau d\sigma \sqrt{-\det h_{\alpha\beta}} \quad (3.6)$$

which describes a trailing string moving with constant velocity [27, 28] in the metric (1.2). Here, h is the metric induced on the string worldsheet.

2. The drag force is given by the momentum flux on the worldsheet of the trailing string along the radial direction, i.e. [27, 28]

$$\frac{dp^i}{dt} = - \left. \frac{\delta S_{NG}}{\delta \partial_\sigma x^i} \right|_{\text{trailing string}} . \quad (3.7)$$

As we will see below, the right-hand side of (3.7) is a conserved quantity on the worldsheet and can be evaluated anywhere on the worldsheet.

3. Denote the retarded propagators for ξ_L and ξ_T as $G_R^{(L)}$ and $G_R^{(T)}$ respectively. Then, the procedure for determining κ_L and κ_T developed in Ref. [25, 26] can be cast as

$$\kappa_{T,L} = - \lim_{\omega \rightarrow 0} \frac{2T_{ws}}{\omega} G_R^{(T,L)}(\omega) , \quad (3.8)$$

where T_{ws} denotes the temperature on the worldsheet. As we will see, the induced metric on the trailing worldsheet has a horizon, meaning that the worldsheet metric can be considered a $(1+1)$ -dimensional black hole. T_{ws} is the Hawking temperature for this worldsheet black hole. Note that at nonzero velocity T_{ws} in general differs from the temperature T of the plasma itself. At zero velocity, the worldsheet horizon coincides with that of the spacetime, while at finite velocity the worldsheet horizon moves closer to the boundary and the corresponding T_{ws} decreases. The reason that one should use the worldsheet temperature rather the spacetime temperature in this computation is that the fluctuations ξ_T (and ξ_L) in the transverse (and longitudinal) directions of the trajectory of the quark moving through the gauge theory plasma arise in the dual gravity description from the fluctuations of the string worldsheet around the trailing string solution [25, 26]. It is as if the force fluctuations that the quark in the boundary gauge theory feels are due to the fluctuations of the string worldsheet to which it is attached.

4. The retarded propagators $G_R^{(L,T)}$ can be found following the general prescription given in [47]. One first solves the linearized equation of motion for the worldsheet fluctuations with the boundary conditions that they are infalling at the worldsheet horizon and go to unity at the ultraviolet boundary. The retarded propagator is then given by the action evaluated on this solution (ignoring possible boundary terms at the horizon).

3.2 Finding the Trailing String and Calculating the Drag

Consider a quark propagating in the x^1 direction with velocity v . In this subsection we shall follow the analysis of Refs. [27, 28] to obtain the corresponding trailing string solution and determine the drag force.

We parametrize the world sheet with t and r and use the ansatz

$$x^1(t, r) = vt + \zeta(r) \quad (3.9)$$

for a late-time steady-state solution. The Nambu-Goto action (3.6) is then

$$S_{NG} = \frac{1}{2\pi\alpha'} \int dt dr \mathcal{L} \quad (3.10)$$

with \mathcal{L} given by

$$\mathcal{L} = e^{\frac{29}{20}c\frac{R^4}{r^2}} \sqrt{1 + \frac{r^4 - r_0^4}{R^4} \zeta'^2 - \frac{v^2 r^4}{r^4 - r_0^4}} , \quad (3.11)$$

where prime denotes differentiation with respect to r . The canonical momentum

$$\pi_\zeta \equiv \frac{\frac{r^4 - r_0^4}{R^4} \zeta'}{\sqrt{1 + \frac{r^4 - r_0^4}{R^4} \zeta'^2 - \frac{v^2 r^4}{r^4 - r_0^4}}} e^{\frac{29}{20}c\frac{R^4}{r^2}} \quad (3.12)$$

is conserved, meaning that

$$\zeta' = \frac{R^4 \pi_\zeta}{r^4 - r_0^4} \sqrt{\frac{r^4 - r_0^4 - v^2 r^4}{(r^4 - r_0^4) e^{\frac{29}{10} c \frac{R^4}{r^2}} - R^4 \pi_\zeta^2}}. \quad (3.13)$$

The integration constant π_ζ can be fixed by the following argument: both the numerator and the denominator of the fraction under the square root in (3.13) are positive at $r = \infty$ and negative at $r = r_0$; since (3.13) is real, both must change sign at the same r ; this is only the case if

$$\pi_\zeta = \frac{r_0^2 v}{R^2 \sqrt{1 - v^2}} e^{\frac{29c\sqrt{1-v^2}R^4}{20r_0^2}}. \quad (3.14)$$

The drag force (3.7) is then

$$\begin{aligned} \frac{dp_1}{dt} &= -\frac{\pi_\xi}{2\pi\alpha'} \\ &= -\frac{\sqrt{\lambda}\pi v T^2}{2\sqrt{1-v^2}} e^{\frac{29c\sqrt{1-v^2}}{20\pi^2 T^2}}, \end{aligned} \quad (3.15)$$

where we have used $R^4 = \lambda\alpha'^2$ and $r_0 = \pi R^2 T$ in the last step. The result (3.15) can also be expressed in terms of the momentum p_1 and mass M of the external quark:

$$\frac{dp_1}{dt} = -\frac{\sqrt{\lambda}\pi T^2}{2} e^{\frac{29c\sqrt{1-v^2}}{20\pi^2 T^2}} \frac{p_1}{M}, \quad (3.16)$$

as obtained previously in Ref. [16]. We see that turning on c increases the drag force, but the effect of the nonconformality becomes weaker at larger v . In fact, for $v \rightarrow 1$ the drag force is independent of c , meaning that in this limit the drag force becomes an infrared insensitive observable. The effects of the nonconformality are largest in the $v \rightarrow 0$ limit: at low velocities, the drag force is increased by a factor of 1.34 (1.80) for $c/T^2 = 2$ ($c/T^2 = 4$). (As was also the case for \hat{q} , the sign of the effect of nonconformality on the drag force is corroborated by the determination that introducing nonzero R -charge chemical potential(s) in $\mathcal{N} = 4$ SYM, which introduces nonconformality, increases the drag force [48].) Finally, notice that when c is nonzero the drag force is not proportional to the momentum. In other words, the drag coefficient $\mu(p_1) \equiv -\frac{1}{p_1} \frac{dp_1}{dt}$ now depends on the velocity and hence on the momentum p_1 .

3.3 Worldsheet Fluctuations

The trailing string solution of Section 3.2 has $x^2 = x^3 = 0$ and so after we change coordinates from r to $z = R^2/r$ it is specified by giving the dependence of x^1 on t and z . Using (3.9) and (3.13), this can be written as

$$\frac{dx^1}{dt} = v \quad (3.17)$$

and

$$\frac{dx^1}{d\bar{z}} = -\frac{\bar{z}^2 v}{1 - \bar{z}^4} e^{\frac{29c(\sqrt{1-v^2}-\bar{z}^2)}{20\pi^2 T^2}} \sqrt{\frac{1 - v^2 - \bar{z}^4}{1 - v^2 - \bar{z}^4 \left(1 - v^2 + v^2 e^{\frac{29c(\sqrt{1-v^2}-\bar{z}^2)}{10\pi^2 T^2}}\right)}}, \quad (3.18)$$

where we have introduced $\bar{z} \equiv z/z_0$.

Following Ref. [26], we now consider small fluctuations around the trailing string solution, which we denote here by x_0^1 , namely

$$x^1 = x_0^1 + \delta x^1(t, z), \quad x^2 = \delta x^2(t, z), \quad x^3 = \delta x^3(t, z). \quad (3.19)$$

We expand the Nambu-Goto action (3.6) to quadratic order in δx^i to obtain

$$S_{NG} = S_{NG}^0 + \frac{R^2}{2\pi\alpha'} \int dt dz \left[\mathcal{G}_L^{\alpha\beta} \partial_\alpha \delta x^1 \partial_\beta \delta x^1 + \sum_{i=2,3} \mathcal{G}_T^{\alpha\beta} \partial_\alpha \delta x^i \partial_\beta \delta x^i \right], \quad (3.20)$$

where S_{NG}^0 is the unperturbed action for the trailing string solution. The quantities $\mathcal{G}_T^{\alpha\beta}$ and $\mathcal{G}_L^{\alpha\beta}$ are given by

$$\mathcal{G}_T^{\alpha\beta} = f_T \sqrt{-h} h^{\alpha\beta}, \quad \mathcal{G}_L^{\alpha\beta} = f_L \sqrt{-h} h^{\alpha\beta}, \quad (3.21)$$

where $h_{\alpha\beta}$ is the induced worldsheet metric whose components we can evaluate using (3.17) and (3.18), obtaining

$$h_{tt} = -\frac{R^2 A \sqrt{1-v^2}}{\hat{z}^2} e^{\frac{29c\sqrt{1-v^2}\hat{z}^2}{20\pi^2 T^2}}, \quad (3.22)$$

$$h_{tz} = h_{zt} = -\frac{R^2 v^2 e^{\frac{29c\sqrt{1-v^2}}{20\pi^2 T^2}}}{1 - (1-v^2)\hat{z}^4} \sqrt{\frac{A}{B}}, \quad (3.23)$$

and

$$h_{zz} = \frac{-e^{\frac{29c\sqrt{1-v^2}(1-\hat{z}^2)}{10\pi^2 T^2}} v^4 \hat{z}^4 + [1 - (1-v^2)\hat{z}^4]^2}{\hat{z}^2 \sqrt{1-v^2} [1 - (1-v^2)\hat{z}^4]^2 B} R^2 e^{\frac{29c\sqrt{1-v^2}\hat{z}^2}{20\pi^2 T^2}}, \quad (3.24)$$

where we have introduced

$$\hat{z} \equiv \sqrt{\gamma} \bar{z} = \sqrt{\gamma} z / z_0 = \sqrt{\gamma} z \pi T, \quad (3.25)$$

with $\gamma \equiv 1/\sqrt{1-v^2}$ and defined

$$A \equiv 1 - \hat{z}^4, \quad (3.26)$$

$$B \equiv 1 - \hat{z}^4 \left[1 - \left(1 - e^{\frac{29c\sqrt{1-v^2}(1-\hat{z}^2)}{10\pi^2 T^2}} \right) v^2 \right], \quad (3.27)$$

and where the prefactors in (3.21) are given by

$$f_T \equiv \frac{e^{\frac{29c\sqrt{1-v^2}\hat{z}^2}{20\pi^2 T^2}}}{2\sqrt{1-v^2}\hat{z}^2} \quad (3.28)$$

$$f_L \equiv \frac{B}{(1-v^2)A} f_T. \quad (3.29)$$

We now make a change of worldsheet coordinates that diagonalizes the worldsheet metric $h_{\alpha\beta}$. This will simplify the calculation since, as is clear from (3.21), diagonalizing $h_{\alpha\beta}$ will also automatically diagonalize \mathcal{G}_T and \mathcal{G}_L . For convenience, we first change coordinates from z to \hat{z} . Then, we define a new coordinate

$$\hat{t} = t + g(\hat{z}) \quad (3.30)$$

where $g(\hat{z})$ satisfies

$$\frac{\partial g}{\partial \hat{z}} = \frac{v^2 \hat{z}^2 e^{\frac{29c\sqrt{1-v^2}(1-\hat{z}^2)}{20\pi^2 T^2}}}{(1-v^2)^{\frac{1}{4}} [1 - (1-v^2)\hat{z}^4] \sqrt{AB}}, \quad (3.31)$$

which ensures that $h_{\hat{t}\hat{z}}$ vanishes. In the new (\hat{z}, \hat{t}) worldsheet coordinate system, the induced worldsheet metric $h_{\hat{\alpha}\hat{\beta}}$ becomes

$$h_{\hat{t}\hat{t}} = -\frac{R^2 A}{\gamma \hat{z}^2} e^{\frac{29c\sqrt{1-v^2}\hat{z}^2}{20\pi^2 T^2}}, \quad (3.32)$$

$$h_{\hat{z}\hat{z}} = \frac{R^2}{\hat{z}^2 B} e^{\frac{29c\sqrt{1-v^2}\hat{z}^2}{20\pi^2 T^2}}. \quad (3.33)$$

We now see that $h_{\hat{t}\hat{t}}$ vanishes and $h_{\hat{z}\hat{z}}$ diverges at $\hat{z} = 1$. This demonstrates that the induced metric on the (1+1)-dimensional worldsheet has an event horizon at $\hat{z} = 1$, corresponding to $z = z_0/\sqrt{\gamma} = 1/(\pi T\sqrt{\gamma})$ and $r = r_0\sqrt{\gamma} = R^2\pi T\sqrt{\gamma}$. Note that the worldsheet horizon moves toward the ultraviolet as $v \rightarrow 1$ and $\gamma \rightarrow \infty$. The $\hat{z} < 1$ region of the worldsheet is outside, and to the ultraviolet of, the worldsheet horizon. The $\hat{z} > 1$ region is inside, and to the infrared. Classically, no signal from the interior of the worldsheet horizon can propagate along the worldsheet to the exterior. The Hawking temperature T_{ws} of the worldsheet black hole is obtained as follows. First, we note that via a change of coordinates, the worldsheet metric outside the horizon, in the vicinity of the horizon, takes the form $ds^2 = -b^2\rho^2 dt^2 + d\rho^2$ for some constant b , where the horizon is at $\rho = 0$. Then, it is a standard argument that in order to avoid having a conical singularity at $\rho = 0$ in the Euclidean version of this metric, $b\hat{t}$ must be a periodic with period 2π . We then identify the period of \hat{t} , namely $2\pi/b$, as $1/T_{ws}$. This argument yields

$$T_{ws} = \frac{T}{\sqrt{\gamma}} \sqrt{1 - \frac{29cv^2\sqrt{1-v^2}}{20\pi^2 T^2}}. \quad (3.34)$$

The diffusion in momentum space of the moving heavy quark, governed by the diffusion constants κ_T and κ_L , is described in the dual gravity theory by the fluctuations of the worldsheet outside the worldsheet horizon due to the worldsheet Hawking radiation with temperature T_{ws} . With T_{ws} in hand, we turn now to the calculation of the diffusion constants (3.8).

3.4 Calculation of κ_T

We now calculate the two point function for the transverse fluctuations, starting from the quantity \mathcal{G}_T defined in (3.20) and given explicitly in Eqs. (3.21)-(3.27) and (3.32) and (3.33). It turns out that it is convenient to define $u \equiv \hat{z}^2$ as the radial coordinate in the calculations of κ_T and κ_L . We write the transverse fluctuations part of the action as

$$S_{NG}^T = \frac{R^2}{2\pi\alpha'} \int dt du [g_1(\partial_t \delta y)^2 + g_2(\partial_u \delta y)^2] , \quad (3.35)$$

where δy here can be either δx_2 or δx_3 and where

$$g_1 \equiv \frac{\mathcal{G}_T^{tt}}{2\sqrt{u}} = -\frac{1}{4u^{\frac{3}{2}}(1-u^2)(1-v^2)^{\frac{3}{4}}\sqrt{AB}} e^{\frac{29cu\sqrt{1-v^2}}{20\pi^2 T^2}} , \quad (3.36)$$

$$g_2 \equiv 2\sqrt{u}\mathcal{G}_T^{\hat{z}\hat{z}} = \frac{\sqrt{AB}}{\sqrt{u}(1-v^2)^{\frac{1}{4}}} e^{\frac{29cu\sqrt{1-v^2}}{20\pi^2 T^2}} , \quad (3.37)$$

and where it is understood that we have rewritten A from (3.26) and B from (3.27) in terms of u , obtaining

$$A = 1 - u^2 , \quad (3.38)$$

$$B = 1 - \left[1 - \left(1 - e^{\frac{29c(1-u)\sqrt{1-v^2}}{10\pi^2 T^2}} \right) v^2 \right] u^2 . \quad (3.39)$$

The equation of motion for the transverse fluctuations δy is given by

$$\partial_u^2 \delta y + \frac{\partial_u g_2}{g_2} \partial_u \delta y + \frac{g_1}{g_2} \partial_t^2 \delta y = 0 . \quad (3.40)$$

After a Fourier transformation

$$\delta y(t, u) = \int_{-\infty}^{\infty} e^{-i\omega t} Y_\omega(u) \frac{d\omega}{2\pi} , \quad (3.41)$$

the equation of motion (3.40) becomes

$$\partial_u^2 Y_\omega + \frac{\partial_u g_2}{g_2} \partial_u Y_\omega - \frac{\omega^2 g_1}{g_2} Y_\omega = 0 . \quad (3.42)$$

To examine the behavior of the solution near the worldsheet horizon $u = 1$, we expand the coefficients in (3.42) near $u = 1$ and obtain

$$\partial_u^2 Y_\omega + \frac{1}{u-1} \partial_u Y_\omega + \frac{\gamma\omega^2}{8(u-1)^2 \left(2 - \frac{29cv^2\sqrt{1-v^2}}{10\pi^2 T^2} \right)} Y_\omega = 0 , \quad (3.43)$$

whose solution is

$$Y_\omega = (1 - u) \pm \frac{i\sqrt{\gamma}\omega}{2\sqrt{4 - \frac{29cv^2\sqrt{1-v^2}}{5\pi^2 T^2}}} . \quad (3.44)$$

For the solution with the “plus” sign, the phase increases as one goes to smaller value of u , i.e. “outward” from the worldsheet horizon, toward the ultraviolet, meaning that this corresponds to an outgoing solution, which is to be discarded in our case. We only need the infalling solution. Therefore, we can write our solution Y_ω as

$$Y_\omega = (1 - u^2) - \frac{i\sqrt{\gamma}\omega}{2\sqrt{4 - \frac{29cv^2\sqrt{1-v^2}}{5\pi^2 T^2}}} F(\omega, u) , \quad (3.45)$$

where $F(\omega, u)$ is regular at the horizon. We now substitute (3.45) into (3.42) and obtain an ordinary differential equation for F that takes the form

$$X F + V \partial_u F + \partial_u^2 F = 0 , \quad (3.46)$$

where X and V are functions of u and ω (that depend on v and T) whose leading behavior at small ω is given explicitly in Appendix A.

In order to determine κ_T , we only need to find the solution F to (3.46) to first order in ω . We show in Appendix A that to zeroth order in ω the only solutions that are regular at the horizon at $u = 1$ are $F = \text{constant}$. We normalize Y_ω so that $Y_\omega \rightarrow 1$ at $u \rightarrow 0$, and this determines that we choose $F = 1$ to zeroth order in ω . To first order in ω the solution then takes the form

$$F = 1 + \omega Z + O(\omega^2) , \quad (3.47)$$

and in Appendix A we show that the function Z has the properties that it goes to a constant at the horizon $u = 1$ and that

$$Z \rightarrow \frac{i}{3} \sqrt{\gamma} e^{\frac{29c\sqrt{1-v^2}}{20\pi^2 T^2}} u^{\frac{3}{2}} + \dots \quad (3.48)$$

as $u \rightarrow 0$. Upon normalizing Y_ω at $u \rightarrow 0$ as we have done, the retarded propagator that appears in (3.8) is given by [47]

$$G_R^T(\omega) = -\frac{R^2(\pi T)^2}{\pi\alpha'} g_2 Y_{-\omega}(u) \partial_u Y_\omega(u) \Big|_{u \rightarrow 0} = -\sqrt{\lambda} \pi T^2 g_2 \omega \partial_u Z(u) \Big|_{u \rightarrow 0} + O(\omega^2) , \quad (3.49)$$

where g_2 is given in (3.37). Using (3.48) and the fact that $g_2 = \frac{1}{(1-v^2)^{\frac{1}{4}} \sqrt{u}} + \mathcal{O}(\sqrt{u})$ in the $u \rightarrow 0$ limit, we find that with the propagator (3.49) and the world sheet temperature (3.34) the transverse momentum diffusion constant (3.8) is given by

$$\kappa_T = \alpha_T \sqrt{\gamma} \sqrt{\lambda} \pi T^3 \quad (3.50)$$

where

$$\alpha_T = e^{\frac{29c\sqrt{1-v^2}}{20\pi^2 T^2}} \sqrt{1 - \frac{29cv^2\sqrt{1-v^2}}{20\pi^2 T^2}} . \quad (3.51)$$

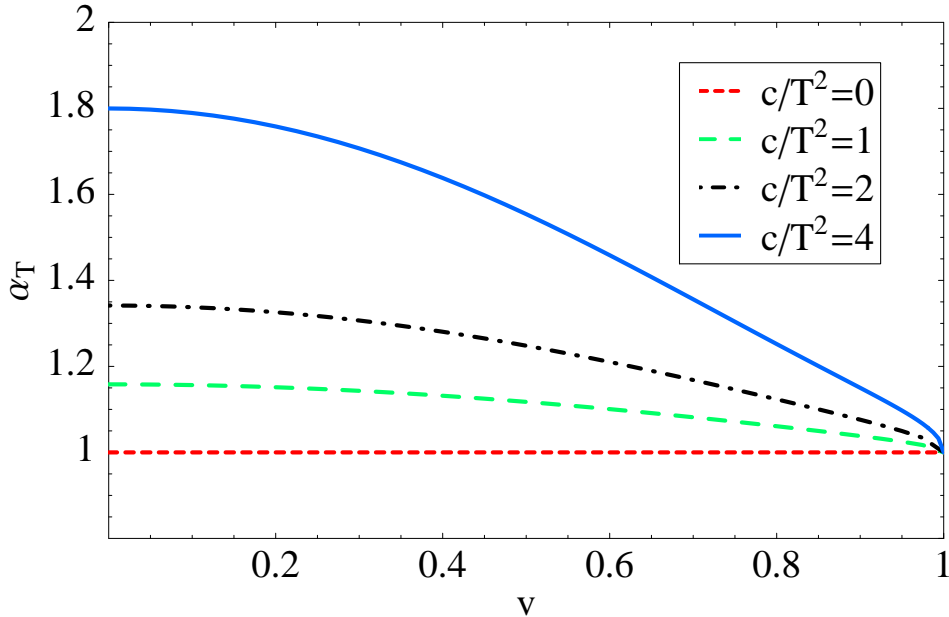


Figure 2: The modification of κ_T due to nonconformality is given by α_T in (3.51), which we plot here versus v at four values of c/T^2 .

When $c = 0$, $\alpha_T = 1$ and our result reduces to the known result for $\mathcal{N} = 4$ SYM, derived in Refs. [25, 26]. From our result, we see that turning on c/T^2 increases κ_T by a factor α_T , which we have plotted in Fig. 2 as a function of v for several values of c/T^2 . Comparing α_T at $v = 0$ from (3.51) to our result (3.16) for the drag coefficient evaluated at $v = 0$, we see that at $v = 0$ the Einstein relation (3.5) is valid with $c \neq 0$. This can be seen as a consistency check on the model.

We see from Fig. 2 that the effect of $c/T^2 = 4$ ($c/T^2 = 2$) on κ_T at low velocity is significant, increasing it by a factor of 1.80 (1.34). This suggests that the nonconformality in QCD could increase the diffusion constant κ_T , which has been related to charm quark energy loss and azimuthal anisotropy in Refs. [46, 49], by a significant factor relative to estimates based upon the $\mathcal{N} = 4$ SYM result. By comparing Fig. 2 to Fig. 1, we also see that at low velocities κ_T is less robust with respect to the introduction of nonconformality than \hat{q} : the effects of c/T^2 on κ_T at low velocity are more than a factor of two larger than its effects on \hat{q} . However, we also see that $\alpha_T \rightarrow 1$ for $v \rightarrow 1$: at high velocities, κ_T does not sense the nonconformality at all. This infrared insensitivity in the high velocity regime can be understood immediately once we recall that the worldsheet horizon is at $z = z_0(1 - v^2)^{1/4}$, and κ_T only depends on the portion of the string worldsheet that is outside the horizon, namely between the ultraviolet boundary at $z = 0$ and $z = z_0(1 - v^2)^{1/4}$. At high velocity, $z_0(1 - v^2)^{1/4}$ itself moves closer and closer toward the boundary, i.e. farther and farther into the ultraviolet, meaning that κ_T only probes ultraviolet physics where c is not important.

3.5 Calculation of κ_L

The calculation of κ_L is analogous to that of κ_T . The relevant action for longitudinal fluctuation

takes the same form as (3.35), with g_1 and g_2 replaced by

$$g_1 = -\frac{1}{4u^{\frac{3}{2}}(1-u^2)(1-v^2)^{\frac{7}{4}}} e^{\frac{29cu\sqrt{1-v^2}}{20\pi^2 T^2}} \sqrt{\frac{B}{A}}, \quad (3.52)$$

$$g_2 = \frac{1-u^2}{\sqrt{u}(1-v^2)^{\frac{5}{4}}} e^{\frac{29cu\sqrt{1-v^2}}{20\pi^2 T^2}} \left(\frac{B}{A}\right)^{\frac{3}{2}}. \quad (3.53)$$

The solution again takes the form (3.45), with F satisfying (3.46), but with different expressions for the functions X and V , given in Appendix A.2. The expansion (3.47) still holds, but now $Z(u)$ can only be obtained numerically. Again, as described in Appendix A, the solution for Z is determined uniquely by requiring that Z be regular at $u = 1$ and that $Z \rightarrow 0$, so that $Y_\omega \rightarrow 1$, as $u \rightarrow 0$. We find that κ_L is given by

$$\kappa_L = 2\gamma^{-\frac{1}{2}} \sqrt{\lambda} \pi T^3 \sqrt{1 - \frac{29cv^2\sqrt{1-v^2}}{20\pi^2 T^2}} g_2 \left(\frac{\partial_u Z}{i} \right) \Big|_{u \rightarrow 0}. \quad (3.54)$$

Near $u = 0$, g_2 can be expanded as $g_2 = \frac{1}{(1-v^2)^{\frac{5}{4}} \sqrt{u}} + \mathcal{O}(\sqrt{u})$, which reduces (3.54) to

$$\kappa_L = \alpha_L \gamma^{\frac{5}{2}} \sqrt{\lambda} \pi T^3, \quad (3.55)$$

where

$$\alpha_L = \frac{2}{\sqrt{\gamma}} \sqrt{1 - \frac{29cv^2\sqrt{1-v^2}}{20\pi^2 T^2}} \left(\frac{\partial_u Z}{i\sqrt{u}} \right) \Big|_{u \rightarrow 0} \quad (3.56)$$

depends on v and c/T^2 . We have checked analytically that $\alpha_L = 1$ for $c = 0$, meaning that our result reduces to that for $\mathcal{N} = 4$ SYM from Refs. [25, 26] when the nonconformality is turned off. That is, α_L is the factor by which κ_L is modified when we introduce nonconformality via nonzero c/T^2 . At nonzero c/T^2 , we compute $Z(u)$ and hence α_L numerically. In Fig. 3 we plot α_L versus v at four values of c/T^2 . The factor α_L is comparable to but somewhat less than its counterpart α_T for the transverse momentum diffusion constant κ_T , plotted in Fig. 2. As $v \rightarrow 0$, α_L and α_T become equal because there is no difference between (diffusion in) longitudinal and transverse momentum when $v = 0$. The effects of c/T^2 on κ_L at small velocity are more than twice as large as its effects on \hat{q} , but κ_L becomes completely unaffected by c/T^2 , namely infrared insensitive, as $v \rightarrow 1$. We also see that there is a range of velocities near 1 for which $\alpha_L < 1$.

3.6 Robustness and Infrared Sensitivity

The effects of the nonconformality we have introduced on all three of the quantities that we have computed that describe the drag and diffusion of a heavy quark moving through the plasma are comparable at low velocities. For $c/T^2 = 1, 2, 4$, the nonconformality serves to increase all three quantities that we have computed, by factors of 1.16, 1.34, 1.80 at $v = 0$. So, particularly at lower temperatures where c/T^2 is larger, the tendency for the drag and diffusion coefficients to increase

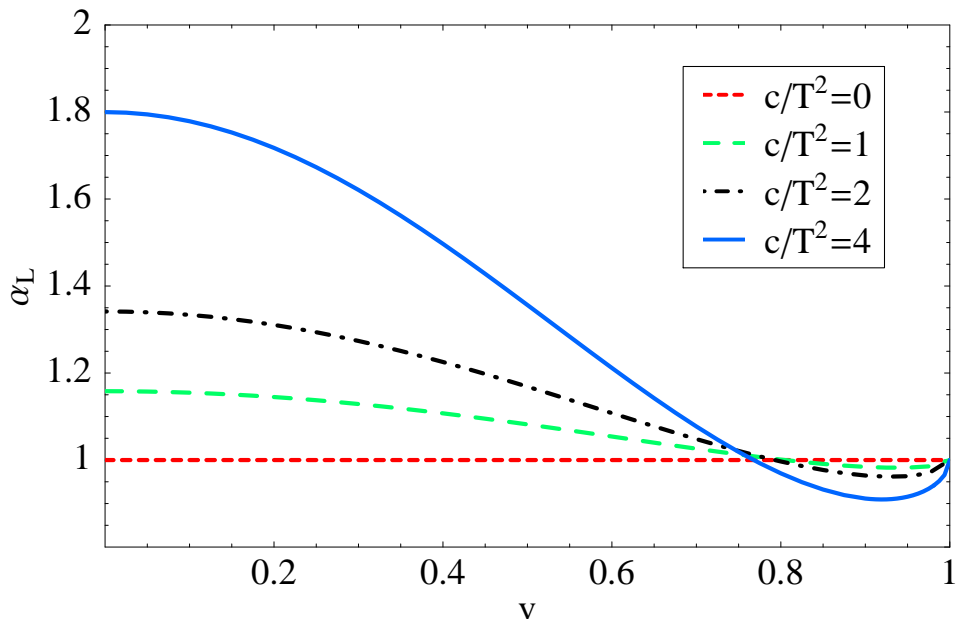


Figure 3: The modification of κ_L due to nonconformality is given by α_L in (3.56), which we plot here versus v at four values of c/T^2 .

with nonconformality should be included in making estimates of these quantities for the QCD plasma. We also showed that the energy loss on a heavy quark moving through the plasma with $v \neq 0$ is not described by a velocity-independent drag coefficient. If we define the drag coefficient $-\frac{1}{p} \frac{dp}{dt}$ then this quantity depends significantly on the velocity of the quark.

All three quantities that we have computed in this section become completely infrared *insensitive* for $v \rightarrow 1$. The $\mathcal{N} = 4$ SYM results for μ , κ_T and κ_L are conventionally quoted in terms of the temperature T , but their infrared insensitivity for $v \rightarrow 1$ demonstrates that in this regime they should really be quoted in terms of z_0 , with z_0 understood as a parameter that specifies the asymptotic ($z \rightarrow 0$) behavior of the metric. In a generic metric that is given asymptotically by the AdS black hole metric (1.1), z_0 is not related in any simple way to the temperature T , which is determined by the metric in the vicinity of the horizon. And, in the $v \rightarrow 1$ regime, μ , κ_T and κ_L are determined by z_0 not by T . The reason for the infrared insensitivity of all three quantities is the same. The drag and diffusion of the quark is described by that segment of the attached string worldsheet that is outside the worldsheet event horizon at $z = z_0(1 - v^2)^{\frac{1}{4}}$. As v approaches 1, this worldsheet event horizon moves to smaller and smaller z , meaning that the segment of the worldsheet that is outside its event horizon, namely at $z < z_0(1 - v^2)^{\frac{1}{4}}$, explores the metric only at smaller and smaller z , meaning that it describes the physics of the more and more ultraviolet sector of the gauge theory. Because the metric that we are using is given asymptotically at small z by the AdS black hole metric (1.1), independent of c , the drag and diffusion of the quark become completely insensitive to c/T^2 for $v \rightarrow 1$. That is, they become infrared insensitive, probing the gauge theory only at more and more ultraviolet scales. We saw in Section 2 that, in contrast, the jet quenching parameter \hat{q} ,

which is defined at $v = 1$, is infrared sensitive.

4. Quark-Antiquark Potential and Screening Length

One of the early, classic, computations done using the AdS/CFT correspondence was the computation of the potential between a static quark and antiquark separated by a distance L in $\mathcal{N} = 4$ SYM theory, first at zero temperature where the potential is Coulomb-like, proportional to $\sqrt{\lambda}/L$ [35], and then at nonzero temperature [36], where, to order $\sqrt{\lambda}$ in the strong coupling expansion, the screened potential is Coulomb-like for $L \ll L_c(T)$ and flat for $L \gg L_c(T)$ (up to order λ^0 contributions that fall exponentially with L [50]). The screening length turns out to be $L_c = 0.24/T$. When $L < L_c(T)$, the potential is determined to order $\sqrt{\lambda}$ at strong coupling by the area of a string worldsheet bounded by the worldlines of the quark and antiquark, with the worldsheet “hanging” into the AdS black hole spacetime (1.1), “suspended” from the test quark and antiquark that are located at the ultraviolet boundary at $z = 0$.

In Refs. [30, 11], the analysis of screening was extended to the case of a quark-antiquark pair moving through the plasma with velocity v . In that context, it proved convenient to define a slightly different screening length L_s , which is the L beyond which no connected extremal string world sheet hanging between the quark and antiquark can be found. At $v = 0$, $L_s = 0.28/T$ [36]. At nonzero v , up to small corrections that have been computed [30, 11],

$$L_s^{\text{meson}}(v, T) \simeq L_s(0, T)(1 - v^2)^{1/4} \propto \frac{1}{T}(1 - v^2)^{1/4} . \quad (4.1)$$

This result, also obtained in [31, 32] and further explored in [51, 52, 53], has proved robust in the sense that it applies in various strongly coupled plasmas other than $\mathcal{N} = 4$ SYM [51, 52, 53], including some which are made nonconformal via the introduction of R-charge chemical potentials. The robustness of the result (4.1) has been tested in a second sense by analyzing the potential and screening length defined by a configuration consisting of N_c external quarks arranged in a circle of radius L , a “baryon”, moving through the strongly coupled plasma [54]. In order to obtain a baryon-like configuration, the N_c strings hanging down into the AdS black hole spacetime must end on a D5-brane [55]. Even with this qualitatively new ingredient, a screening length once again emerges naturally, and obeys (4.1) for “baryons” moving through the plasma [54]. The velocity dependence of the screening length (4.1) suggests that in a theory containing dynamical heavy quarks and meson bound states (which $\mathcal{N} = 4$ SYM does not) the dissociation temperature $T_{\text{diss}}(v)$, defined as the temperature above which mesons with a given velocity do not exist, should scale with velocity as [30]

$$T_{\text{diss}}(v) \simeq T_{\text{diss}}(v = 0)(1 - v^2)^{1/4} , \quad (4.2)$$

since $T_{\text{diss}}(v)$ should be the temperature at which the screening length $L_s^{\text{meson}}(v)$ is comparable to the size of the meson bound state. The scaling (4.2) indicates that slower mesons can exist up to higher temperatures than faster ones, a result which has observable consequences for charmonium (bottomonium) production as a function of transverse momentum in heavy ion collisions at RHIC (LHC) [30, 11]. This result has proved robust in a third sense, in that (4.2) has also been

obtained by direct analysis of the dispersion relations of actual mesons in the plasma [56, 57], introduced by adding heavy quarks described in the gravity dual by a D7-brane whose fluctuations are the mesons [58, 56, 57]. These mesons have a limiting velocity whose temperature dependence is equivalent to (4.2), up to few percent corrections that have been computed [57].

In this section, we shall return to the velocity-dependent screening length defined by a quark-antiquark pair moving through the plasma and test the robustness of (4.1) in yet one more way by repeating the calculation of $L_s(v, T)$ from Refs. [30, 11] in the metric (1.2) that incorporates the nonconformal deformation whose consequences we are exploring throughout the present paper.

4.1 Calculating the Potential

Consider an external quark-antiquark dipole moving with velocity $v = \tanh \eta$, where η is the rapidity of the dipole, along the $-x_3$ direction. We choose the quark and antiquark to be separated by a distance L , oriented in the x_1 direction. It proves convenient to boost into a frame in which the dipole is at rest in a moving medium — it feels a “hot wind” — via a Lorentz transformation $(t, x_3) \rightarrow (t', x'_3)$:

$$dt = dt' \cosh \eta - dx'_3 \sinh \eta \quad (4.3)$$

$$dx_3 = -dt' \sinh \eta + dx'_3 \cosh \eta . \quad (4.4)$$

In the dipole rest frame, the spacetime metric describing the nonconformal hot wind is obtained by applying the Lorentz transformation to the metric (1.2), obtaining

$$ds^2 = \frac{R^2}{z^2} e^{\frac{29cz^2}{20}} \left\{ \left[\sinh^2 \eta - \left(1 - \frac{z^4}{z_0^4} \right) \cosh^2 \eta \right] dt'^2 + \left[\cosh^2 \eta - \left(1 - \frac{z^4}{z_0^4} \right) \sinh^2 \eta \right] dx_3'^2 - 2 \frac{z^4}{z_0^4} \sinh \eta \cosh \eta dt' dx'_3 + dx_1^2 + dx_2^2 + \frac{dz^2}{1 - \frac{z^4}{z_0^4}} \right\} . \quad (4.5)$$

To evaluate the potential between a static quark and antiquark in this background we first need to evaluate the action of a rectangular time-like Wilson loop whose long sides, of length \mathcal{T} , are aligned with the t' axis and whose short sides, of length L , are oriented in the x_1 direction. We then need to subtract the action of a separated quark and antiquark, each trailing a string described as in Section 3.2.

To evaluate the Nambu-Goto action of the string worldsheet bounded by the rectangular Wilson loop that describes the moving dipole, we parametrize the string worldsheet by $\tau = t'$ and $\sigma = x_1 \in [-\frac{L}{2}, \frac{L}{2}]$. The spacetime coordinates of the worldsheet are then given by $(\tau, \sigma, 0, 0, z(\sigma))$, and its Nambu-Goto action (3.6) is

$$S_{\text{NG}}^{\text{dipole}} = \frac{R^2 \mathcal{T}}{2\pi\alpha'} \int_{-\frac{L}{2}}^{\frac{L}{2}} d\sigma \frac{e^{\frac{29cz^2}{20}}}{z^2} \sqrt{\left[-\sinh^2 \eta + \left(1 - \frac{z^4}{z_0^4} \right) \cosh^2 \eta \right] \left(1 + \frac{z'^2}{1 - \frac{z^4}{z_0^4}} \right)} , \quad (4.6)$$

where we have denoted $\partial_\sigma z$ by z' . We must extremize this action in order to determine $z(\sigma)$, subject to the boundary conditions $z(\pm\frac{L}{2}) = 0$. Note that $z(\sigma)$ is symmetric about $\sigma = 0$, which is where

$z(\sigma)$ reaches its maximum value which we shall denote z_* . Note also that the integration over $[-\frac{L}{2}, 0]$ is the same as $[0, \frac{L}{2}]$. With a change of variables, the action (4.6) can be expressed as an integral over z :

$$S_{\text{NG}}^{\text{dipole}} = \frac{R^2 \mathcal{T}}{\pi \alpha'} \int_0^{z_*} dz \mathcal{L} \quad (4.7)$$

with the Lagrangian

$$\mathcal{L} = \frac{e^{-\frac{29cz^2}{20}}}{z^2} \sqrt{\left[-\sinh^2 \eta + \left(1 - \frac{z^4}{z_0^4}\right) \cosh^2 \eta \right] \left(\frac{1}{z'^2} + \frac{1}{1 - \frac{z^4}{z_0^4}} \right)}. \quad (4.8)$$

Since the Lagrangian has no explicit dependence on σ , the corresponding Hamiltonian

$$\begin{aligned} \mathcal{H} &= z' \frac{\partial \mathcal{L}}{\partial z'} - \mathcal{L} \\ &= -\frac{e^{-\frac{29cz^2}{20}}}{z^2} \sqrt{\frac{\left[-\sinh^2 \eta + \left(1 - \frac{z^4}{z_0^4}\right) \cosh^2 \eta \right] \left(1 - \frac{z^4}{z_0^4}\right)}{1 - \frac{z^4}{z_0^4} + z'^2}} \end{aligned} \quad (4.9)$$

is ‘‘conserved’’, by which we mean that it is independent of z . In particular,

$$\mathcal{H}(z) = \mathcal{H}(z_*) = -\frac{e^{-\frac{29cz_*^2}{20}}}{z_*^2} \sqrt{-\sinh^2 \eta + \left(1 - \frac{z_*^4}{z_0^4}\right) \cosh^2 \eta}, \quad (4.10)$$

where in the evaluation of $\mathcal{H}(z_*)$ we have used the fact that $z' = 0$ at $z = z_*$. We can now rearrange (4.9) and (4.10) to obtain an expression for z' , namely

$$z' = \pm \sqrt{\left(1 - \frac{z^4}{z_0^4}\right) \left(\frac{q(z_*)}{q(z)} - 1\right)}, \quad (4.11)$$

where the $+$ ($-$) sign applies for $-L/2 \leq \sigma \leq 0$ (for $0 \leq \sigma \leq L/2$) and where we have defined

$$q(z) \equiv \frac{e^{-\frac{29cz^2}{10}} z^4 z_0^4}{z_0^4 - z^4 \cosh^2 \eta}. \quad (4.12)$$

Upon substituting (4.11) into (4.7), we find

$$S_{\text{NG}}^{\text{dipole}} = \frac{\sqrt{\lambda} \mathcal{T}}{\pi} \int_0^{z_*} dz \frac{e^{-\frac{29cz^2}{20}}}{z^2} \sqrt{\frac{\left(1 - \frac{z^4}{z_0^4}\right) \cosh^2 \eta - \sinh^2 \eta}{\left(1 - \frac{z^4}{z_0^4}\right) \left(1 - \frac{q(z)}{q(z_*)}\right)}}, \quad (4.13)$$

where we have used $R^2/\alpha' = \sqrt{\lambda}$.

The action (4.13) is written in terms of z_* , the turning point of the string worldsheet, rather than in terms of L , the separation between the quark and antiquark. L and z_* are related by

$$\begin{aligned} \frac{L}{2} &= \int_0^{z_*} \frac{dz}{z'} \\ &= \int_0^{z_*} \frac{dz}{\sqrt{\left(1 - \frac{z^4}{z_0^4}\right) \left(\frac{q(z_*)}{q(z)} - 1\right)}} . \end{aligned} \quad (4.14)$$

We will express our results in terms of L

The action (4.13) contains not only the potential between the quark-antiquark pair but also the (infinite) masses of the quark and antiquark considered separately in the moving medium. We must therefore subtract the (infinite) action $2S_{\text{NG}}^0$ of two independent quarks, namely

$$E(L)\mathcal{T} = S_{\text{NG}}^{\text{dipole}} - 2S_{\text{NG}}^0 , \quad (4.15)$$

in order to extract the potential $E(L)$. The string configuration corresponding to a single quark at rest in the moving medium is obtained from the trailing string solution described in our analysis of heavy quark drag in Section 3.2 by substituting (3.13) and (3.14) into (3.10) and (3.11), changing variables from r to z , and boosting to the frame in which the quark is at rest and the plasma is moving. We find

$$S_{\text{NG}}^0 = \frac{\sqrt{\lambda}\mathcal{T}}{2\pi} \int_0^{z_0} dz \frac{e^{\frac{29 cz^2}{10}}}{z^2} \sqrt{\frac{z^4 \cosh^2 \eta - z_0^4}{e^{\frac{29 cz^2}{10}} (z^4 - z_0^4) + e^{\frac{29 cz_0^2}{10 \cosh \eta}} z^4 \sinh^2 \eta}} . \quad (4.16)$$

Finally, the quark-antiquark potential $E(L)$ is obtained by substituting (4.16) and (4.13) into (4.15) and using (4.14) to relate z_* to L . We have checked that for $c = 0$ these expressions all reduce to those in Ref. [11].

In order to make a plot of $E(L)$, we use (4.13) and (4.14) to evaluate E and L at a series of values of the parameter z_* , performing the integrals numerically. Then, in Fig. 4 we plot $E/(\sqrt{\lambda}\mathcal{T})$ versus $L\pi T$ for four values of the nonconformality c/T^2 , for a quark-antiquark pair moving with rapidity $\eta = 1$. Each curve has two branches that meet at a cusp, with the cusp occurring at $L = L_s$, the largest value of L at which a string worldsheet connecting the quark and antiquark can be found. The lower branch is the potential of interest. The upper branch describes unstable string configurations [59]. Two branches arise because $L(z_*)$ in (4.14) is not monotonic: every value of $L < L_s$ is obtained at two different values of z_* . For $L > L_s$, $E/\sqrt{\lambda}$ vanishes. We therefore identify L_s as the screening length. (At low velocities this introduces a small imprecision since $E(L_s)$ is just positive and the screening length should then be identified as the L at which the lower branch crosses $E = 0$.)

4.2 Robustness and Infrared Sensitivity of the Screening Length

In Fig. 5, we illustrate the velocity dependence of the screening length L_s for four values of the nonconformality c/T^2 . We have plotted $L_s\pi T\sqrt{\cosh \eta}$; to the degree that the curves are flat, we

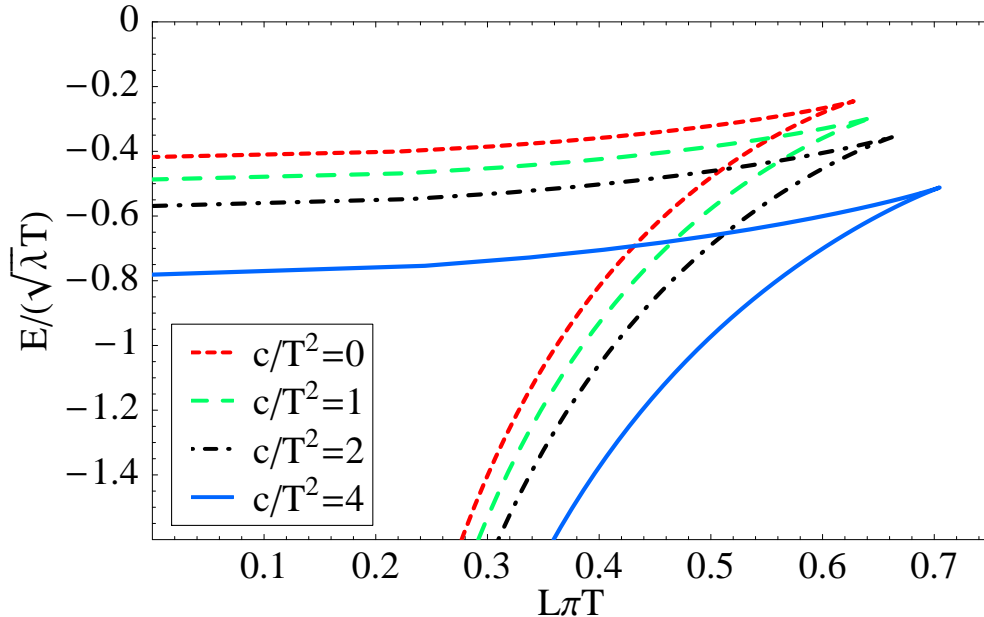


Figure 4: The potential $E(L)$ between a quark and antiquark moving through the plasma with rapidity $\eta = 1$, for four different values of the nonconformity c/T^2 . We plot $E/(\sqrt{\lambda}T)$ versus $L\pi T$. Each curve has two branches that meet at a cusp at $L = L_s$, with the lower branch being the potential of interest. For each curve, the maximum possible L at which a string worldsheet connecting the quark and antiquark can be found occurs at the cusp, $L = L_s$.

can conclude that the velocity dependence is $L_s\pi T \propto 1/\sqrt{\cosh\eta} = (1 - v^2)^{1/4}$ as in (4.1). We see from the figure that this is the leading velocity dependence at large η , as can also be demonstrated analytically [11]. And, we see that this leading dependence describes the velocity dependence to within corrections of order 20% all the way down to $v = 0$. These conclusions hold for $c \neq 0$ as for $c = 0$, although the corrections at small velocity grow somewhat, meaning that we have successfully tested the robustness of the velocity scaling (4.1) against the introduction of nonconformity via c/T^2 .

If we now look at the effects of c/T^2 on the value of L_s , not just on its leading velocity dependence, we see that turning on the nonconformity parameter results in a modest increase in L_s . The effect is greatest at $v = 0$, but even there L_s increases by only about 20% for $c/T^2 = 4$. This means that, among the five observables that we have analyzed and within the model we have employed, L_s is the most robust against the introduction of nonconformity. At large velocities, L_s becomes completely c -independent, meaning that at large velocities it is infrared insensitive. This can be understood as follows. In order for the right-hand side of (4.10) to be real, the turning point of the string worldsheet z_* , and thus the entire worldsheet, must lie somewhere within $0 \leq z \leq z_0/\sqrt{\cosh\eta} = z_0(1 - v^2)^{1/4}$. This means that in the high velocity limit, the string worldsheet only probes the the small- z , ultraviolet, region of the metric where the effects of c are not felt. To put it more simply, since as $v \rightarrow 1$ the screening length shrinks, $L_s\pi T \propto (1 - v^2)^{1/4}$, the

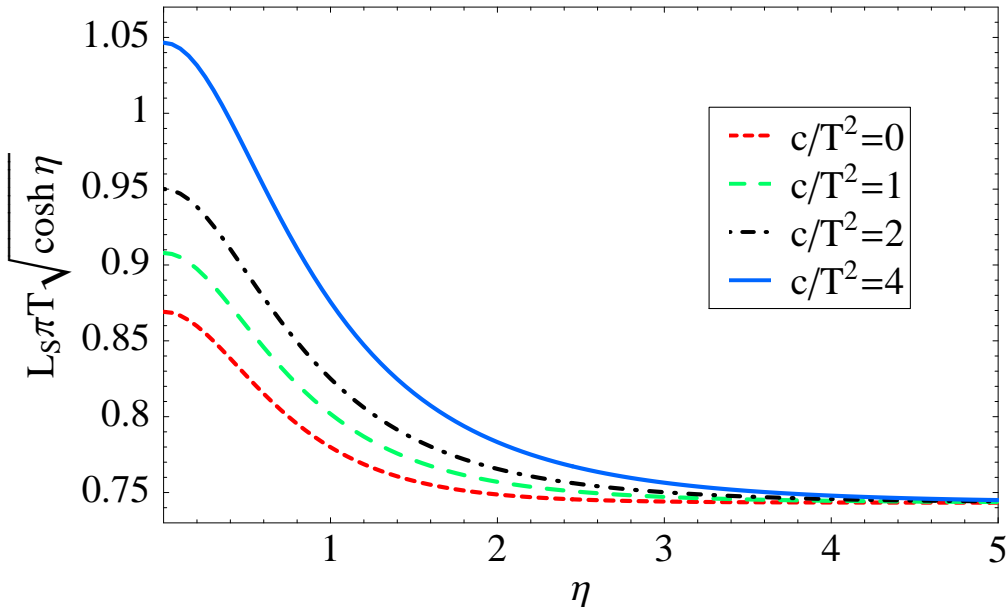


Figure 5: $L_s \pi T \sqrt{\cosh \eta}$ versus rapidity η at four values of c/T^2 .

quark-antiquark dipole becomes sensitive only to more and more ultraviolet physics of the plasma.

The authors of Ref. [51] have shown that in the cascading gauge theory of Refs. [40, 12] L_s is affected by the introduction of nonconformality even at large velocity. This does not contradict our conclusion that L_s becomes infrared insensitive at high velocity because this theory includes nonconformality at all scales, not just in the infrared.⁵ Furthermore, the meson dispersion relations analyzed in Refs. [56, 57] indicate that the size of the largest stable mesons moving through the plasma with a given velocity shrinks with increasing velocity in the same way that L_s shrinks,⁶ indicating that if the meson dispersion relations were to be studied in a nonconformal model like the one that we have analyzed, they too would become infrared insensitive for mesons moving with high velocity.

We have seen that in addition to being the leading velocity dependence of L_s for $v \rightarrow 1$, the

⁵Our results may provide a counterexample to a conjecture made in Refs. [51, 53]. Upon writing $L_s \propto (1 - v^2)^p$, these authors suggested the relationship $(\frac{1}{4} - p) \propto (\frac{1}{3} - v_s^2)$, where v_s is the velocity of sound. We find $p = \frac{1}{4}$, but v_s^2 is almost certainly not $\frac{1}{3}$ with $c \neq 0$. Firm conclusions cannot be drawn, however, since, as explained in Ref. [17] and Section 1, we cannot compute thermodynamic quantities like v_s reliably in the model we are employing because the deformed metric (1.2) is not a solution to supergravity equations of motion.

⁶The mesons are described by fluctuations of a D7-brane. Stable mesons moving through the plasma with a given velocity v can be found for a range of quark masses M extending upward from some minimum possible M/T . The fluctuations corresponding to stable mesons with the smallest possible M/T for a given v turn out to be well localized in z at the value of z corresponding to the point where the D7-brane gets closest to the black hole. According to the standard holographic relationship between position in z and scale in the gauge theory, the location in z of this “tip” of the D7-brane therefore corresponds to the size in the gauge theory of the largest stable mesons with a given propagation velocity v . The results of Ref. [56, 57] show that this size decreases with increasing velocity proportional to $(1 - v^2)^{1/4}$, just like the screening length L_s .

expression $L_s \pi T \propto (1 - v^2)^{1/4}$ provides a reasonable description at all velocities. This velocity dependence can have consequences for the p_T -dependence of charmonium (bottomonium) production in heavy ion collisions at RHIC (LHC), as it suggests that if temperatures close to but below that at which a particular quarkonium species dissociates at rest are achieved, the production of this species would drop for p_T above some threshold [30, 11]. In this context, the quarkonium velocities that are relevant will not be particularly close to $v \rightarrow 1$, meaning that L_s in the relevant regime will not be infrared insensitive.

5. Outlook

We have found that the drag and momentum diffusion constants that describe a heavy quark moving through the strongly coupled plasma and the screening length for a quark-antiquark pair moving through the plasma all become infrared insensitive as $v \rightarrow 1$. Although we used a particular toy model to diagnose this fact, in each case we can understand it as a consequence of intrinsic attributes of the quantity in question, meaning that the conclusion of infrared insensitivity at high velocity transcends the particular model. In the case of the screening length, at high velocity it becomes small which means that in the $v \rightarrow 1$ limit it only probes the ultraviolet physics of the plasma. (In the regime of velocities accessible to quarkonium mesons produced in heavy ion collisions, the screening length retains some infrared sensitivity.) In the case of the drag and momentum diffusion constants, at high velocity they are determined in their dual gravity description by the shape and fluctuations of that portion of their trailing string worldsheet that is outside, namely to the ultraviolet of, a worldsheet horizon that itself moves farther and farther into the ultraviolet as the quark velocity increases. In the limit of high velocity, all four of these quantities are only sensitive to the short distance physics of the plasma, namely to physics in a regime where the $\mathcal{N} = 4$ SYM plasma is strongly coupled but the quark-gluon plasma in QCD is not. The jet quenching parameter, on the other hand, is infrared sensitive even though it is defined at $v = 1$. Again, this arises from an intrinsic attribute of the quantity in question, in this case the fact that in its dual gravity description the jet quenching parameter is defined by a string worldsheet that extends all the way from the ultraviolet boundary of the metric at $z = 0$ to the black hole horizon and thus probes physics of the plasma at all scales down to of order the temperature.

Our investigation of their infrared sensitivity provides a new illustration of the qualitative distinction between the momentum diffusion constants κ_T and κ_L on the one hand and the jet quenching parameter \hat{q} on the other, which arise when two noncommuting limits are taken in opposite orders [11, 60]. We have already noted that κ_T and κ_L are only well-defined at $v \rightarrow 1$ if we take this limit while satisfying the criterion (1.4), for example by taking the $M \rightarrow \infty$ limit first. If the $M \rightarrow \infty$ limit is taken before the $v \rightarrow 1$ limit (more generally, if (1.4) is satisfied), the quark trajectories for which κ_T and κ_L are defined are always timelike, even as $v \rightarrow 1$. On the other hand, \hat{q} is determined by a strictly light-like Wilson loop. (The light-like Wilson lines should be thought of as describing trajectories of the gluons radiated from the hard parton that is losing energy as it traverses the medium.) We can introduce a quark mass M as an ultraviolet regulator in the definition of the Wilson loop. Then, in order to define a light-like Wilson loop in the gauge theory we must first take $v \rightarrow 1$, and only then take the regulator $M \rightarrow \infty$, since if we took the

limits in the opposite order the Wilson loop would not be light-like. Our investigations show that \hat{q} , defined via the light-like Wilson loop, is infrared sensitive: it probes the properties of the strongly coupled plasma at all scales down to those of order the temperature. In contrast, if one tries to push κ_T and κ_L to $v \rightarrow 1$ while satisfying (1.4) one obtains observables that are only sensitive to the ultraviolet physics of the plasma, where $\mathcal{N} = 4$ SYM is unlikely to be a good guide to QCD.

It would be a significant advance to find other ratios of observables that are (even close to) as universal as η/s , which is the same for all gauge theories with dual gravity descriptions in the strong coupling and large- N_c limit. Finding infrared sensitive observables is a prerequisite, since no infrared insensitive observable can be universal. Both η and s are infrared sensitive quantities; their ratio turns out to be universal. Our results suggest two further infrared sensitive observables: the jet quenching parameter \hat{q} , defined at $v = 1$, and the $v = 0$ drag coefficient and momentum diffusion constant, which are related by (3.5). It is an open question whether there are ratios involving either of these observables that are universal.

If we take as a benchmark value $c/T^2 = 4$, which corresponds to about twice the level of nonconformality indicated by lattice QCD calculations of the conformal anomaly $\varepsilon - 3P$ at $T \sim 300$ MeV, we find that turning on this level of nonconformality in the model spacetime (1.2) that we have analyzed increases the jet quenching parameter by about 30%, increases the quark-antiquark screening length by about 20% at low velocity, and increases the heavy quark drag, transverse momentum diffusion, and longitudinal momentum diffusion all by about 80%, again at low velocity. The effects of nonconformality on the latter four quantities all vanish at high velocities, as discussed above. The possibility of a significant enhancement in the transverse momentum diffusion constant at low velocity introduced by turning on a degree of nonconformality comparable to that in QCD thermodynamics should be taken into account in future comparisons to charm quark energy loss and azimuthal anisotropy as in Refs. [46, 49]. Note also that the drag coefficient is no longer a velocity-independent constant when nonconformality is turned on, decreasing by almost a factor of two as v is increased from near zero to near one with $c/T^2 = 4$. The fact that the slowing of a moving heavy quark is no longer governed simply by $dp/dt \propto -p$ in a strongly coupled but nonconformal plasma generalizes beyond the toy model context within which we have discerned it.

Our evaluation of the robustness of the five quantities we have computed against the introduction of nonconformality can serve as a partial and qualitative guide to estimating how these quantities change in going from $\mathcal{N} = 4$ SYM to QCD. A more complete understanding requires studying the effects of changing the number of degrees of freedom in addition to introducing nonconformality. And, our results for robustness are only quantitatively valid within the model in which we have obtained them, making it important to perform analyses like ours in other contexts in which nonconformality can be turned on. Both these lines of thought serve as strong motivation for carrying out a study like the one in this paper for the plasma of strongly coupled $\mathcal{N} = 2^*$ gauge theory [13].

Acknowledgments

We acknowledge helpful conversations with Christiana Athanasiou, Jorge Casalderrey-Solana, Qudsia Ejaz, Tom Faulkner, Steven Gubser, David Mateos, Eiji Nakano, Makoto Natsuume, Derek Teaney

and Urs Wiedemann. HL is supported in part by the A. P. Sloan Foundation and the U.S. Department of Energy (DOE) OJI program. YS is supported in part by the MIT Undergraduate Research Opportunity Program. This research was supported in part by the DOE Offices of Nuclear and High Energy Physics under grants #DE-FG02-94ER40818 and #DE-FG02-05ER41360.

A. Some Technical Details

A.1 Technical Details Needed in the Calculation of κ_T

In Section 3.4, we calculate the transverse momentum diffusion constant κ_T by determining the two point function for the transverse fluctuations of the worldsheet of the trailing string. The equation of motion for the Fourier transform of the transverse fluctuations, Y_ω , is given in (3.42), and solutions with the correct behavior (3.45) near the horizon $u = 1$ are then specified by the ordinary differential equation (3.46) for $F(\omega, u)$, defined in (3.45). The differential equation (3.46) contains two functions X and V that we did not specify in Section 3.4. To lowest order in ω , these functions are given by

$$X = X_1 \omega + \mathcal{O}(\omega^2) , \quad (\text{A.1})$$

and

$$V = V_0 + \mathcal{O}(\omega) , \quad (\text{A.2})$$

where

$$\begin{aligned} X_1 = & - \frac{i \sqrt{\gamma}}{20 \pi (1 - u^2)^2 \sqrt{4 \pi^2 - \frac{29 c v^2 \sqrt{1 - v^2}}{5 T^2}}} \left\{ -40 \pi^2 u^2 - 20 \pi^2 (1 - u^2) \right. \\ & + \frac{1}{T^2 \left[-u^2 v^2 + e^{-\frac{29 c (1 - u) \sqrt{1 - v^2}}{10 \pi^2 T^2}} (1 - u^2 (1 - v^2)) \right]} \left[10 \pi^2 T^2 u^2 (1 - 3u^2) v^2 \right. \\ & \left. \left. - e^{-\frac{29 c (1 - u) \sqrt{1 - v^2}}{10 \pi^2 T^2}} \left(29 c u (1 - u^2) (1 - u^2 (1 - v^2)) \sqrt{1 - v^2} \right. \right. \right. \\ & \left. \left. \left. - 10 \pi^2 T^2 (1 + u^2 (2 - v^2) - 3 u^4 (1 - v^2)) \right) \right] \right\} \quad (\text{A.3}) \end{aligned}$$

and

$$\begin{aligned} V_0 = & - \frac{1}{20 \pi^2 T^2 u (1 - u^2) \left(-u^2 v^2 + e^{-\frac{29 c (1 - u) \sqrt{1 - v^2}}{10 \pi^2 T^2}} (1 - u^2 (1 - v^2)) \right)} \left\{ 10 \pi^2 T^2 u^2 (1 - 3u^2) v^2 \right. \\ & \left. - e^{-\frac{29 c (1 - u) \sqrt{1 - v^2}}{10 \pi^2 T^2}} \left[29 c u (1 - u^2) (1 - u^2 (1 - v^2)) \sqrt{1 - v^2} \right. \right. \\ & \left. \left. - 10 \pi^2 T^2 (1 + u^2 (2 - v^2) - 3 u^4 (1 - v^2)) \right] \right\} . \quad (\text{A.4}) \end{aligned}$$

In this Appendix, we shall solve the equation (3.46) for F , first to zeroth order in ω and then to first order.

To zeroth order in ω , (3.46) reads

$$V_0 \partial_u F + \partial_u^2 F = 0 . \quad (\text{A.5})$$

We can solve this equation upon noticing that near $u = 1$, V_0 can be expanded in powers of $(1 - u)$ and takes on the simple form

$$V_0 = -\frac{1}{1 - u} + \mathcal{O}(1) . \quad (\text{A.6})$$

This means that the only solutions to (A.5) that are regular at $u = 1$ are constant solutions, with $\partial_u F = 0$. Normalizing Y_ω such that $Y_\omega \rightarrow 1$ in the $u \rightarrow 0$ limit corresponds to choosing the constant solution $F = 1$. This normalization is required if one is to preserve the standard AdS/CFT relationship between the fluctuations of the string worldsheet in the bulk, δy , and operators and sources in the gauge theory on the boundary at $u = 0$. In particular, it is required in order for the retarded propagator G_R to be given by (3.49). The same normalization is also used in the calculation of κ_L .

Now, working to first order in ω and knowing that $F = 1$ to zeroth order, we write F as

$$F = 1 + \omega Z , \quad (\text{A.7})$$

a form that we used in (3.47). The first order terms in the differential equation (3.46) then become

$$X_1 + V_0 \partial_u Z + \partial_u^2 Z = 0 . \quad (\text{A.8})$$

We now define

$$W \equiv -i \partial_u Z , \quad (\text{A.9})$$

and obtain a first order differential equation for $W(u)$ given by

$$\frac{X_1}{i} + V_0 W + \partial_u W = 0 , \quad (\text{A.10})$$

where X_1 and V_0 are given by (A.3) and (A.4). Note that since X_1 is imaginary the equation (A.10) for W has real coefficients. The differential equation (A.10) can be solved analytically, yielding

$$\begin{aligned} W = & - \frac{\sqrt{u} \sqrt{\gamma}}{(1 - u^2) \sqrt{20 \pi^2 - \frac{29 c v^2 \sqrt{1 - v^2}}{T^2}} \sqrt{e^{-\frac{29 c \sqrt{1 - v^2}}{10 \pi^2 T^2}} \left(-e^{\frac{29 c \sqrt{1 - v^2}}{10 \pi^2 T^2}} u^2 v^2 + e^{\frac{29 c u \sqrt{1 - v^2}}{10 \pi^2 T^2}} (1 - u^2 (1 - v^2)) \right)}} \\ & \times \left\{ \pi \sqrt{5 u e^{-\frac{29 c \sqrt{1 - v^2}}{10 \pi^2 T^2}} \left(-e^{\frac{29 c \sqrt{1 - v^2}}{10 \pi^2 T^2}} u^2 v^2 + e^{\frac{29 c u \sqrt{1 - v^2}}{10 \pi^2 T^2}} (1 - u^2 (1 - v^2)) \right)} \right. \\ & \left. + C \sqrt{1 - u^2} \sqrt{20 \pi^2 - \frac{29 c v^2 \sqrt{1 - v^2}}{T^2}} \right\} , \quad (\text{A.11}) \end{aligned}$$

where the integration constant C has to be determined by the requirement that W must be regular at the worldsheet horizon $u = 1$. To determine C , we expand (A.11) about $u = 1$, which yields

$$W = \frac{\sqrt{\gamma} \left(C + \frac{1}{2}\right) \pi}{\sqrt{4\pi^2 - \frac{29cv^2\sqrt{1-v^2}}{5T^2}}} \frac{1}{u-1} + \mathcal{O}(1) \quad (\text{A.12})$$

The coefficient of the $1/(u-1)$ term in (A.12) must vanish, which determines that $C = -\frac{1}{2}$. With C determined, (A.11) constitutes a fully explicit expression for W , which according to (A.9) should then be integrated to give Z . The further integration constant in Z is fixed by the requirement that $Y_\omega \rightarrow 1$, meaning that $Z \rightarrow 0$, for $u \rightarrow 0$. In our calculation of κ_T , we do not need the entire function Z . According to (3.49), all we need is the leading term in Z (or W) at $u \rightarrow 0$. From (A.11) we determine that $W \propto \sqrt{u}$ in the $u \rightarrow 0$ limit, and upon integrating to determine Z in this regime we obtain (3.48).

A.2 Technical Details Needed in the Calculation of κ_L

The technical details needed in the calculation of κ_L are completely analogous to those described in Appendix A.1, including in particular the logic of how the boundary conditions are satisfied. The only difference is in the functions X_1 and V_0 , which in the longitudinal case are given by

$$\begin{aligned} X_1 = & - \frac{i\sqrt{\gamma}}{20\pi(1-u)^2 \sqrt{4\pi^2 - \frac{29cv^2\sqrt{1-v^2}}{5T^2}}} \left\{ -40\pi^2 u^2 - 20\pi^2(1-u^2) \right. \\ & + \frac{1}{T^2 \left(-u^2 v^2 + e^{-\frac{29c(1-u)\sqrt{1-v^2}}{10\pi^2 T^2}} (1-u^2(1-v^2)) \right)} \left[10\pi^2 u^2 v^2 T^2 (5-3u^2) \right. \\ & \quad - 58cu^3 v^2 (1-u^2) \sqrt{1-v^2} \\ & \quad \left. \left. - e^{-\frac{29c(1-u)\sqrt{1-v^2}}{10\pi^2 T^2}} \left(29cu(1-u^2) \sqrt{1-v^2} (1-u^2(1-v^2)) \right) \right] \right\} \\ & \left. + 30\pi^2 u^4 T^2 (1-v^2) - 10\pi^2 T^2 (1+u^2(2-5v^2)) \right\}, \quad (\text{A.13}) \end{aligned}$$

and

$$\begin{aligned}
V_0 = & - \frac{1}{20 \pi^2 T^2 u (1 - u^2) \left(-u^2 v^2 + e^{-\frac{29 c (1-u) \sqrt{1-v^2}}{10 \pi^2 T^2}} (1 - u^2 (1 - v^2)) \right)} \\
& \times \left\{ 2u^2 v^2 \left(5\pi^2 T^2 (5 - 3u^2) - 29 cu (1 - u^2) \sqrt{1 - v^2} \right) \right. \\
& \quad \left. - e^{-\frac{29 c (1-u) \sqrt{1-v^2}}{10 \pi^2 T^2}} \left[29 cu (1 - u^2) \sqrt{1 - v^2} (1 - u^2 (1 - v^2)) \right. \right. \\
& \quad \left. \left. - 10 \pi^2 T^2 \left(1 + u^2 (2 - 5v^2) - 3u^4 (1 - v^2) \right) \right] \right\}. \quad (\text{A.14})
\end{aligned}$$

References

- [1] J. M. Maldacena, *Adv. Theor. Math. Phys.* **2**, 231 (1998) [*Int. J. Theor. Phys.* **38**, 1113 (1999)] [arXiv:hep-th/9711200]; E. Witten, *Adv. Theor. Math. Phys.* **2**, 253 (1998) [arXiv:hep-th/9802150]; S. S. Gubser, I. R. Klebanov and A. M. Polyakov, *Phys. Lett. B* **428**, 105 (1998) [arXiv:hep-th/9802109]; O. Aharony, S. S. Gubser, J. M. Maldacena, H. Ooguri and Y. Oz, *Phys. Rept.* **323**, 183 (2000) [arXiv:hep-th/9905111].
- [2] L. Susskind and E. Witten, arXiv:hep-th/9805114; A. W. Peet and J. Polchinski, *Phys. Rev. D* **59**, 065011 (1999) [arXiv:hep-th/9809022].
- [3] K. Adcox *et al.* [PHENIX Collaboration], *Nucl. Phys. A* **757**, 184 (2005) [arXiv:nucl-ex/0410003]; B. B. Back *et al.* [PHOBOS Collaboration], *Nucl. Phys. A* **757**, 28 (2005) [arXiv:nucl-ex/0410022]; I. Arsene *et al.* [BRAHMS Collaboration]; *Nucl. Phys. A* **757**, 1 (2005) [arXiv:nucl-ex/0410020]; J. Adams *et al.* [STAR Collaboration], *Nucl. Phys. A* **757**, 102 (2005) [arXiv:nucl-ex/0501009].
- [4] G. Boyd, J. Engels, F. Karsch, E. Laermann, C. Legeland, M. Lutgemeier and B. Petersson, *Nucl. Phys. B* **469**, 419 (1996) [arXiv:hep-lat/9602007]; F. Karsch, E. Laermann and A. Peikert, *Phys. Lett. B* **478**, 447 (2000) [arXiv:hep-lat/0002003]; A. Ali Khan *et al.* [CP-PACS collaboration], *Phys. Rev. D* **64**, 074510 (2001) [arXiv:hep-lat/0103028]; Y. Aoki, Z. Fodor, S. D. Katz and K. K. Szabo, *JHEP* **0601**, 089 (2006) [arXiv:hep-lat/0510084].
- [5] M. Cheng *et al.*, *Phys. Rev. D* **77**, 014511 (2008) [arXiv:0710.0354 [hep-lat]].
- [6] Z. Fodor, arXiv:0711.0336 [hep-lat].
- [7] For reviews, see F. Karsch, *Nucl. Phys. A* **698**, 199 (2002) [arXiv:hep-ph/0103314]; F. Karsch, *J. Phys. Conf. Ser.* **46**, 122 (2006) [arXiv:hep-lat/0608003]; F. Karsch, *Nucl. Phys. A* **783**, 13 (2007) [arXiv:hep-ph/0610024].
- [8] G. Policastro, D. T. Son and A. O. Starinets, *Phys. Rev. Lett.* **87**, 081601 (2001) [arXiv:hep-th/0104066].

- [9] P. Kovtun, D. T. Son and A. O. Starinets, *JHEP* **0310**, 064 (2003) [arXiv:hep-th/0309213].
- [10] A. Buchel and J. T. Liu, *Phys. Rev. Lett.* **93**, 090602 (2004) [arXiv:hep-th/0311175]; A. Buchel, *Phys. Lett. B* **609**, 392 (2005) [arXiv:hep-th/0408095].
- [11] H. Liu, K. Rajagopal and U. A. Wiedemann, *JHEP* **0703**, 066 (2007) [arXiv:hep-ph/0612168].
- [12] A. Buchel, C. P. Herzog, I. R. Klebanov, L. A. Pando Zayas and A. A. Tseytlin, *JHEP* **0104**, 033 (2001) [arXiv:hep-th/0102105]; S. S. Gubser, C. P. Herzog, I. R. Klebanov and A. A. Tseytlin, *JHEP* **0105**, 028 (2001) [arXiv:hep-th/0102172].
- [13] A. Buchel and J. T. Liu, *JHEP* **0311**, 031 (2003) [arXiv:hep-th/0305064]; A. Buchel, *Nucl. Phys. B* **708**, 451 (2005) [arXiv:hep-th/0406200]; A. Buchel, S. Deakin, P. Kerner and J. T. Liu, *Nucl. Phys. B* **784**, 72 (2007) [arXiv:hep-th/0701142].
- [14] A. Karch, E. Katz, D. T. Son and M. A. Stephanov, *Phys. Rev. D* **74**, 015005 (2006) [arXiv:hep-ph/0602229].
- [15] C. P. Herzog, *Phys. Rev. Lett.* **98**, 091601 (2007) [arXiv:hep-th/0608151].
- [16] E. Nakano, S. Teraguchi and W. Y. Wen, *Phys. Rev. D* **75**, 085016 (2007) [arXiv:hep-ph/0608274].
- [17] K. Kajantie, T. Tahkokallio and J. T. Yee, *JHEP* **0701**, 019 (2007) [arXiv:hep-ph/0609254].
- [18] H. Liu, K. Rajagopal and U. A. Wiedemann, *Phys. Rev. Lett.* **97**, 182301 (2006) [arXiv:hep-ph/0605178].
- [19] A. Buchel, *Phys. Rev. D* **74**, 046006 (2006) [arXiv:hep-th/0605178].
- [20] R. Baier, Y. L. Dokshitzer, A. H. Mueller, S. Peigne and D. Schiff, *Nucl. Phys. B* **484** (1997) 265 [arXiv:hep-ph/9608322].
- [21] B. G. Zakharov, *JETP Lett.* **63** (1996) 952 [arXiv:hep-ph/9607440]; *JETP Lett.* **65**, 615 (1997) [arXiv:hep-ph/9704255].
- [22] U. A. Wiedemann, *Nucl. Phys. B* **588**, 303 (2000) [arXiv:hep-ph/0005129].
- [23] M. Gyulassy, P. Levai and I. Vitev, *Nucl. Phys. B* **594**, 371 (2001) [arXiv:nucl-th/0006010]; B. G. Zakharov, *JETP Lett.* **73**, 49 (2001) [*Pisma Zh. Eksp. Teor. Fiz.* **73**, 55 (2001)] [arXiv:hep-ph/0012360]; X. N. Wang and X. f. Guo, *Nucl. Phys. A* **696**, 788 (2001) [arXiv:hep-ph/0102230]; C. A. Salgado and U. A. Wiedemann, *Phys. Rev. D* **68**, 014008 (2003) [arXiv:hep-ph/0302184]; S. Jeon and G. D. Moore, *Phys. Rev. C* **71**, 034901 (2005) [arXiv:hep-ph/0309332].
- [24] For reviews, see R. Baier, D. Schiff and B. G. Zakharov, *Ann. Rev. Nucl. Part. Sci.* **50**, 37 (2000) [arXiv:hep-ph/0002198]; R. Baier, *Nucl. Phys. A* **715**, 209 (2003) [arXiv:hep-ph/0209038]; M. Gyulassy, I. Vitev, X. N. Wang and B. W. Zhang, arXiv:nucl-th/0302077; A. Kovner and U. A. Wiedemann, arXiv:hep-ph/0304151; P. Jacobs and X. N. Wang, *Prog. Part. Nucl. Phys.* **54**, 443 (2005) [arXiv:hep-ph/0405125]; J. Casalderrey-Solana and C. A. Salgado, arXiv:0712.3443 [hep-ph].

- [25] S. S. Gubser, Nucl. Phys. B **790**, 175 (2008) [arXiv:hep-th/0612143].
- [26] J. Casalderrey-Solana and D. Teaney, arXiv:hep-th/0701123.
- [27] C. P. Herzog, A. Karch, P. Kovtun, C. Kozcaz and L. G. Yaffe, JHEP **0607**, 013 (2006) [arXiv:hep-th/0605158].
- [28] S. S. Gubser, Phys. Rev. D **74**, 126005 (2006) [arXiv:hep-th/0605182].
- [29] J. Casalderrey-Solana and D. Teaney, Phys. Rev. D **74**, 085012 (2006) [arXiv:hep-ph/0605199].
- [30] H. Liu, K. Rajagopal and U. A. Wiedemann, Phys. Rev. Lett. **98**, 182301 (2007) [arXiv:hep-ph/0607062].
- [31] K. Peeters, J. Sonnenschein and M. Zamaklar, Phys. Rev. D **74**, 106008 (2006) [arXiv:hep-th/0606195].
- [32] M. Chernicoff, J. A. Garcia and A. Guijosa, JHEP **0609**, 068 (2006) [arXiv:hep-th/0607089].
- [33] F. Carminati *et al.* [ALICE Collaboration], J. Phys. G **30**, 1517 (2004); B. Alessandro *et al.* [ALICE Collaboration], J. Phys. G **32**, 1295 (2006); D. d'Enterria *et al.* [CMS Collaboration], J. Phys. G **34**, 2307 (2007). H. Takai, [for the ATLAS Collaboration] Eur. Phys. J. C **34**, S307 (2004).
- [34] R. Baier and D. Schiff, JHEP **0609**, 059 (2006) [arXiv:hep-ph/0605183].
- [35] J. M. Maldacena, Phys. Rev. Lett. **80**, 4859 (1998) [arXiv:hep-th/9803002]; S. J. Rey and J. T. Yee, Eur. Phys. J. C **22**, 379 (2001) [arXiv:hep-th/9803001].
- [36] S. J. Rey, S. Theisen and J. T. Yee, Nucl. Phys. B **527**, 171 (1998) [arXiv:hep-th/9803135]; A. Brandhuber, N. Itzhaki, J. Sonnenschein and S. Yankielowicz, Phys. Lett. B **434**, 36 (1998) [arXiv:hep-th/9803137]; J. Sonnenschein, arXiv:hep-th/0003032.
- [37] Z. t. Liang, X. N. Wang and J. Zhou, arXiv:0801.0434 [hep-ph].
- [38] E. Caceres and A. Guijosa, JHEP **0612**, 068 (2006) [arXiv:hep-th/0606134]; F. L. Lin and T. Matsuo, Phys. Lett. B **641**, 45 (2006) [arXiv:hep-th/0606136]; S. D. Avramis and K. Sfetsos, JHEP **0701**, 065 (2007) [arXiv:hep-th/0606190]; N. Armesto, J. D. Edelstein and J. Mas, JHEP **0609**, 039 (2006) [arXiv:hep-ph/0606245].
- [39] J. F. Vazquez-Poritz, arXiv:hep-th/0605296.
- [40] I. R. Klebanov and M. J. Strassler, JHEP **0008**, 052 (2000) [arXiv:hep-th/0007191].
- [41] Early extractions of \hat{q} in comparison with RHIC data include K. J. Eskola, H. Honkanen, C. A. Salgado and U. A. Wiedemann, Nucl. Phys. A **747**, 511 (2005) [arXiv:hep-ph/0406319]; and A. Dainese, C. Loizides and G. Paic, Eur. Phys. J. C **38**, 461 (2005) [arXiv:hep-ph/0406201]. For the current status, see A. Adare *et al.* [PHENIX Collaboration], arXiv:0801.4020 [nucl-ex]; and references therein.
- [42] H. Liu, K. Rajagopal and U. Wiedemann in S. Abreu *et al.*, arXiv:0711.0974 [hep-ph].
- [43] P. C. Argyres, M. Edalati and J. F. Vazquez-Poritz, JHEP **0701**, 105 (2007) [arXiv:hep-th/0608118].

- [44] P. C. Argyres, M. Edalati and J. F. Vazquez-Poritz, *JHEP* **0704**, 049 (2007) [arXiv:hep-th/0612157].
- [45] P. C. Argyres, M. Edalati and J. F. Vazquez-Poritz, arXiv:0801.4594 [hep-th].
- [46] G. D. Moore and D. Teaney, *Phys. Rev. C* **71**, 064904 (2005) [arXiv:hep-ph/0412346].
- [47] D. T. Son and A. O. Starinets, *JHEP* **0209**, 042 (2002) [arXiv:hep-th/0205051].
- [48] C. P. Herzog, *JHEP* **0609**, 032 (2006) [arXiv:hep-th/0605191]; E. Caceres and A. Guijosa, arXiv:hep-th/0605235;
- [49] A. Adare *et al.* [PHENIX Collaboration], *Phys. Rev. Lett.* **98**, 172301 (2007) [arXiv:nucl-ex/0611018].
- [50] D. Bak, A. Karch and L. G. Yaffe, *JHEP* **0708**, 049 (2007) [arXiv:0705.0994 [hep-th]].
- [51] E. Caceres, M. Natsuume and T. Okamura, *JHEP* **0610**, 011 (2006) [arXiv:hep-th/0607233].
- [52] S. D. Avramis, K. Sfetsos and D. Zoakos, arXiv:hep-th/0609079.
- [53] M. Natsuume and T. Okamura, *JHEP* **0709**, 039 (2007) [arXiv:0706.0086 [hep-th]].
- [54] C. Athanasiou, H. Liu and K. Rajagopal, arXiv:0801.1117 [hep-th].
- [55] E. Witten, *JHEP* **9807**, 006 (1998) [arXiv:hep-th/9805112]; D. J. Gross and H. Ooguri, *Phys. Rev. D* **58**, 106002 (1998) [arXiv:hep-th/9805129]; A. Brandhuber, N. Itzhaki, J. Sonnenschein and S. Yankielowicz, *JHEP* **9807**, 020 (1998) [arXiv:hep-th/9806158].
- [56] D. Mateos, R. C. Myers and R. M. Thomson, *JHEP* **0705**, 067 (2007) [arXiv:hep-th/0701132].
- [57] Q. J. Ejaz, T. Faulkner, H. Liu, K. Rajagopal and U. A. Wiedemann, arXiv:0712.0590 [hep-th].
- [58] A. Karch and E. Katz, *JHEP* **0206**, 043 (2002) [arXiv:hep-th/0205236]; M. Kruczenski, D. Mateos, R. C. Myers and D. J. Winters, *JHEP* **0307**, 049 (2003) [arXiv:hep-th/0304032]; J. Babington, J. Erdmenger, N. J. Evans, Z. Guralnik and I. Kirsch, *Phys. Rev. D* **69**, 066007 (2004) [arXiv:hep-th/0306018]; M. Kruczenski, D. Mateos, R. C. Myers and D. J. Winters, *JHEP* **0405**, 041 (2004) [arXiv:hep-th/0311270]; R. C. Myers and R. M. Thomson, *JHEP* **0609**, 066 (2006) [arXiv:hep-th/0605017]; D. Mateos, R. C. Myers and R. M. Thomson, *Phys. Rev. Lett.* **97**, 091601 (2006) [arXiv:hep-th/0605046]; C. Hoyos, K. Landsteiner and S. Montero, *JHEP* **0704**, 031 (2007) [arXiv:hep-th/0612169]; R. C. Myers, A. O. Starinets and R. M. Thomson, *JHEP* **0711**, 091 (2007) [arXiv:0706.0162 [hep-th]]; K. Peeters and M. Zamaklar, *JHEP* **0801**, 038 (2008) [arXiv:0711.3446 [hep-th]]; J. Erdmenger, N. Evans, I. Kirsch and E. Threlfall, arXiv:0711.4467 [hep-th].
- [59] J. J. Friess, S. S. Gubser, G. Michalogiorgakis and S. S. Pufu, *JHEP* **0704**, 079 (2007) [arXiv:hep-th/0609137]; S. D. Avramis, K. Sfetsos and K. Siampos, *Nucl. Phys. B* **769**, 44 (2007) [arXiv:hep-th/0612139]; S. D. Avramis, K. Sfetsos and K. Siampos, *Nucl. Phys. B* **793**, 1 (2008) [arXiv:0706.2655 [hep-th]].
- [60] H. Liu, *J. Phys. G* **34**, S361 (2007) [arXiv:hep-ph/0702210].